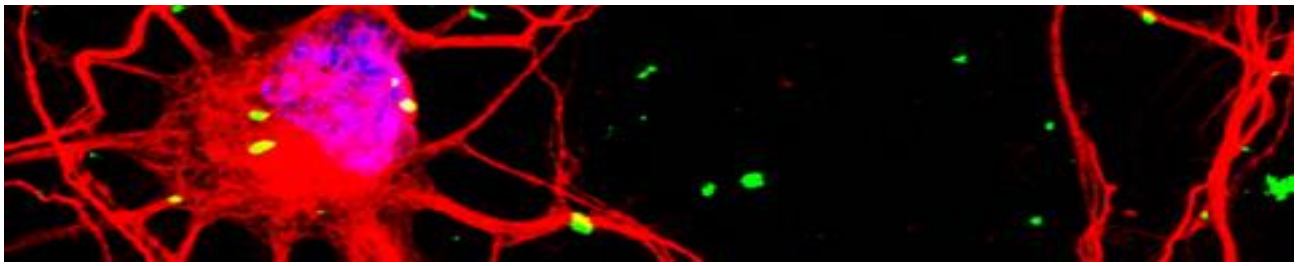

Università degli Studi di Genova

PhD Course in Neuroscience

Curriculum Neuroscience and Neurotechnologies

Cycle XXXIII

Investigating the effect of *Depdc5* cKO: insights on synaptic transmission, plasticity and its role in mTOR-related epilepsy

Candidate:

Maria Sabina Cerullo

Supervisor:

Prof. Fabio Benfenati

ISTITUTO ITALIANO
DI TECNOLOGIA

UNIVERSITÀ DEGLI STUDI
DI GENOVA

“Que dois-je devenir ?

- Un curieux.

- Ce n'est pas un métier.

- Ce n'est pas *encore* un métier. Voyagez, écrivez, apprenez à vivre partout. Commence tout de suite. *L'avenir est au curieux de profession*."

Jules et Jim, François Truffaut

Contents

1. Summary

Focal Epilepsy (FE) accounts for more than the half of the total cases of all epileptic syndrome, around 60%. It can be caused by either genetic or acquired factors, such as brain trauma, tumors or inflammation. However, it is widely recognized to have a mostly a genetic basis. Mutations at the level of the GATOR1 complex components, DEPDC5, NPRL2 and NPRL3, were found in patients with FE, confirming the key role of the GATOR1 complex in the pathogenesis of various FE syndromes. In particular, it has been discovered that mutations of *DEPDC5* gene are implicated in the 5%–37% of a broad range of FEs, both lesional or non-lesional and are associated with mTOR hyperactivity. The specific mechanism underlying the epileptogenic phenotype following *DEPDC5* loss is far from being clear. The aim of this thesis is to deepen the impact of Depdc5 loss-of-function at the cellular level, by focusing the attention on synaptic transmission and plasticity. In order to overcome the problem of embryonic lethality of *Depdc5* full knockout in rodents, and the failure of *Depdc5* constitutive heterozygous knockout mice to recapitulate the major epileptogenic traits, we used *Depdc5*-floxed mice and applied the Cre/LoxP technique to generate a model of *Depdc5* cKO. We transfected primary cortical neurons obtained from *Depdc5*-floxed mice with lentiviruses expressing either active or inactive Cre recombinase and performed electrophysiological and biochemical experiments. We observed an increased in excitatory synaptic transmission and intrinsic excitability, while no difference occurred at the level of the inhibitory synaptic

transmission. Given the involvement of mTOR in the mechanism of plasticity and the effect of its dysregulation on synaptic transmission, we assessed whether *Depdc5* loss could also have an impact at the level of the short-term plasticity (STP). However, no effects were found at the level of either excitatory or inhibitory synaptic transmission. The data suggest that *Depdc5* loss mostly induces a strengthening of excitatory transmission at the post-synaptic level and by increasing the number of connections, without directly affecting pre-synaptic mechanisms. Thus, the enhanced excitatory synaptic transmission and increased intrinsic excitability could generate a synergistic effect underlying the excitation/inhibition imbalance that triggers the epileptogenic process.

2. Introduction

2.1 Epilepsy: the history of a worldwide disease

Epilepsy is one of the most diffuse and disabling neurological disorders, affecting 50 million people worldwide. Before the first modern classification by Henri Gastaut in 1970, seizures and the different epileptic diseases were not distinctly recognized. Gastaut, at the time Secretary-General of ILAE (International League Against Epilepsy) and member of the Commission an Classification, firstly defined the international recognized system and terminology that is still used and has evolved over the years (Gastaut, 1970).

Thanks to the new advances in the neuroimaging, genomic technologies and molecular biology, this classification system underwent several changes and additions. Indeed, thanks to EEG recordings, which had a great impact on the clinical practice, ILAE published in 1981 a first classification of seizures, followed by updates of the epilepsy classification in 1985 and 1989, where the concept of an epilepsy syndrome was introduced (Pack, 2019). Later, another revision occurred in 2010 (Berg et al., 2010), with the final aim of an accepted definitive epilepsy classification, but a full *consensus* was difficult to reach. Thus, in 2014, ILAE assembled a new task force, which developed and published a new definition of epilepsy (Fisher et al., 2014) and in 2017 the final classification of seizures and the epilepsies (Fisher et al., 2017; Scheffer et al., 2017).

Compared to the 1980s classifications, the latest ILAE revised classification contains

modifications and several important additions to improve its intuitiveness, transparency and versatility, fundamental for creating a more efficient and effective communication between patients, their families, clinicians, and researchers (Falco-Walter et al., 2018; Pack, 2019).

2.2 Defining and classifying seizure, epilepsy and epileptic syndromes

The epileptic seizure is define as “a transient occurrence of signs and/or symptoms due to abnormal excessive or synchronous neuronal activity in the brain” (Fisher et al., 2017). The manifestation of excessive and hypersynchronous excitation of neuronal population leads to the transformation of the normal brain rhythms. Epilepsy is present in a patient when recurrent and unprovoked seizures occur (Fisher et al., 2014). Three main criteria have to be considered for epilepsy diagnosis:

1) The patient should suffer from one or at least two unprovoked or reflex seizure less than 24h apart.
2) One unprovoked or reflex seizure and a probability of further seizures similar to the general recurrence risk (> 60%) after two unprovoked seizures, in the next 10 years.
3) An epilepsy syndrome (Fisher et al., 2014).

Some people can experience an epilepsy syndrome, referred to a group of clinical characteristics that consistently occur together, with similar seizure types, age of onset,

EEG results, triggering factors that can be genetics or not, natural history, prognosis, and response to antiepileptic drugs (AEDs) (Stafstrom & Carmant, 2015).

One can also heal from epilepsy, although it is not guarantee that it will not return. In particular, epilepsy is defined resolved when: (i) a patient who had an age-dependent epilepsy syndrome and who is older than the age in which the syndrome is active; or (ii) a patient who did not present any seizure for more than a 10 years and has been off all antiseizure medications for more than 5 years (Falco-Walter et al., 2018).

2.2.1 Classification

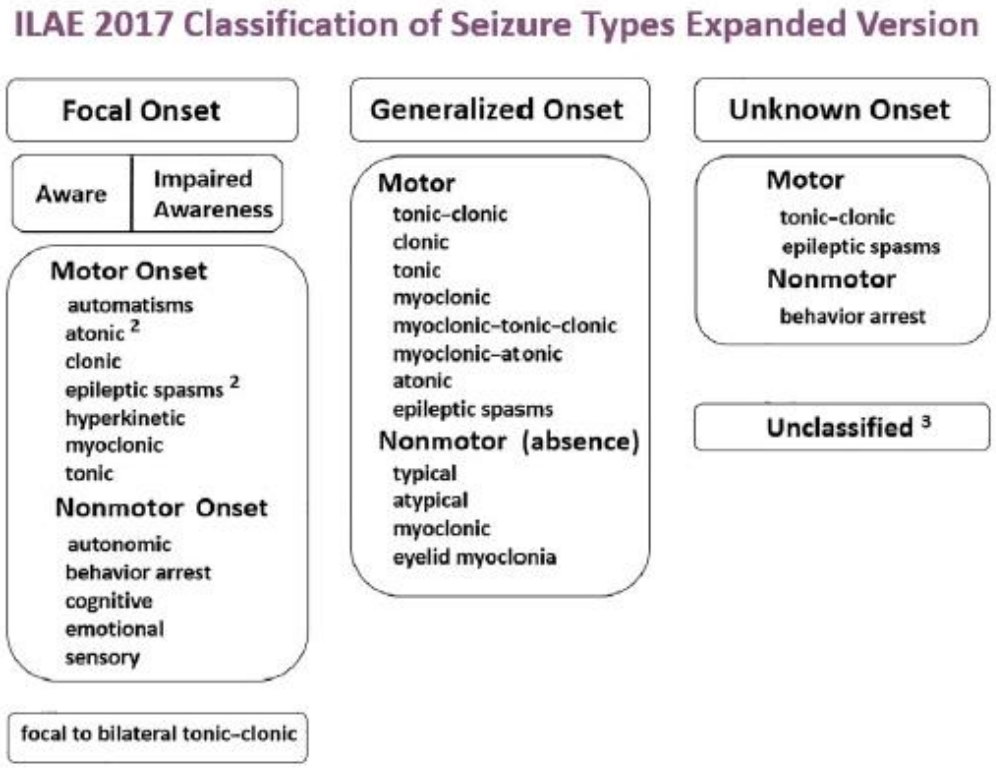

Figure 1. The ILAE 2017 operational classification of seizure types. (from Fisher et al., 2017).

Except for neonatal seizures, seizure classification can be applied to adults and children. The first distinction is according to the onset of seizures. They can be divided into focal, generalized or unknown seizures. A seizure is generalized when it originates at some point within the brain and rapidly distributes in bilateral networks in both hemispheres, whereas a focal seizure originates within a neuronal network in one hemisphere. When the onset of the seizure is ambiguous or unclear, but other manifestations are present, the seizure is of unknown onset (Falco-Walter et al., 2018). Another important feature of a seizure is awareness. It is particularly relevant for focal seizure, since during a generalized seizure awareness is impaired and is omitted in the generalized seizure classification. If awareness is impaired during any part of the seizure, we can classify the event as a focal impaired awareness seizure. For what concerns focal seizures, we can subclassify them according to the presence of motor and non-motor signs and symptoms at the onset. Usually, motor signs are dominating compared to non-motor signs. This is also true for generalized seizures, that can be classified into motor and non-motor. In particular, the generalized motor seizure can be further subclassified into tonic-clonic or other motor. The same classification is applied to unknown onset seizure (Pack, 2019).

2.2.2.1 Generalized seizures

In a case of generalized epilepsy diagnosis, the patient would typically show generalized spike-wave activity on EEG. In particular, according to motor signs, generalized seizures can be distinguished into tonic-clonic, other motor seizures or non-motor generalized

seizures, indicating absence seizures. The diagnosis of generalized epilepsy is made on the basis of clinical evidence, supported by the finding of typical interictal EEG discharges (Falco-Walter et al., 2018; Scheffer et al., 2017).

2.2.2.2 Focal Seizures

One of the features for a first classification of focal epilepsy is patient's awareness, meaning if the patient has knowledge and understanding of what is happening in his/her surroundings during the seizure. If during the seizure awareness is impaired, the event is classified as a focal seizure with impaired awareness. Another important aspect to consider is the motor or non-motor signs at the onset of the event. These early prominent features are important to consider when localizing the seizure onset or epileptogenic zone (Pack, 2019). The interictal EEG typically shows focal epileptiform discharges, but the diagnosis is made on clinical grounds, supported by EEG findings (Scheffer et al., 2017).

2.2.2.3 Unknown seizures

When the patient has epilepsy and all the related symptoms, but the type of epilepsy is difficult to determine, the term "unknown" is used. This could happen because of lack of information, no access to EEG or the EEG studies have been uninformative (Scheffer et al., 2017). Nevertheless, according to motor signs, seizures of unknown onset can be classified as motor or non-motor; otherwise, if information is insufficient, the seizure is considered unclassified (Pack, 2019).

2.2.2 Epilepsy etiology

The causes of seizure onset can be different. The ILAE identified six etiologic categories: structural; genetic; infectious; metabolic; immune; unknown. Sometimes more than one cause can underlie the etiology of the seizure.

1. Structural etiology: when a different structural condition or disease is thought to be the cause of seizures. These abnormalities can be visible through neuroimaging techniques and, together with electroclinical assessments, can be indicated as the likely cause of patient's seizure. Structural lesions can be acquired by a stroke, trauma or infection event, or can have a genetic origin, like in tuberous sclerosis and malformation of cortical development (Falco-Walter et al., 2018; Scheffer et al., 2017).

2. Genetic etiology: when epilepsy seems to be the direct result of a known or presumed genetic disorder in which seizures are the main manifestations. To contribute to epilepsy pathogenesis can be de novo mutations or copy number variations. However, the identification of the genetic etiology can be challenging, especially with many patients having variants of unknown significance (Falco-Walter et al., 2018).

3. Infectious etiology: it refers to a patient presenting epilepsy, not a patient with seizures due to an acute infection. Neurocysticercosis, HIV, CMV and cerebral toxoplasmosis can be considered infectious etiologies, many of which could also be considered as a structural etiology (Falco-Walter et al., 2018).

4. Metabolic epilepsies: refers to a patient with epilepsy which is due to a metabolic derangement (Scheffer et al., 2017)

5. Immune etiology: when an autoimmune disease is the cause of epilepsy onset. An example is antibody-mediated limbic encephalitis, which is an increasingly recognized cause of seizures in epilepsies of unknown origin (Falco-Walter et al., 2018)

6. Unknown category: refers to epilepsy whose etiology remains unclear (Falco-Walter et al., 2018).

2.3 Mechanisms of epileptogenesis and solutions for treating epilepsy

Understanding the cellular and molecular mechanisms underlying the epileptogenic process is a fundamental step for developing new and effective therapies against epilepsy.

Epileptogenesis occurs when a pathogenic event transforms physiological neuronal circuits into hyperexcitable circuits, disrupting their normal activity and leading to epileptic condition. Epileptogenesis acts at various levels in both neuronal and non-neuronal cells in the brain, ranging from genetic and epigenetic alterations to molecular and structural changes (Devinsky et al., 2018). During epileptogenesis, transcription of voltage-gated and receptor-gated ion channels is altered. For example, transcription of low threshold T-type calcium channels, such as Cav3.2 channels, is enhanced, inducing seizure during epileptogenesis. Interestingly, after genetic deletion of the gene in *status epilepticus*-exposed mice or pharmacological inhibition of T-type calcium channel by ethosuximide, spontaneous seizures, spike and wave discharges are decreased (Dezsi et al., 2013). Mutations in voltage-gated sodium channels also play an important role in epileptogenesis. Loss-of-function mutations in $Na_V1.1$ cause Severe Myoclonic Epilepsy of Infancy (Dravet Syndrome). Mice with loss-of-function mutations in $Na_V1.1$ channels show a strong impairment of sodium currents and action potential firing in hippocampal GABAergic inhibitory neurons, but with no notable effect on the excitatory pyramidal neurons, thus leading to hyperexcitability and seizures (Catterall, 2013). During

epileptogenesis, gene expression is also altered through epigenetic mechanisms such as DNA methylation, histone modification and microRNA (miRNA) expression. Gene activation occurs through DNA hypomethylation within 1 day of experimental *status epilepticus,* whereas gene silencing induced by DNA hypermethylation has been observed in chronic epilepsy models and in patients with TLE (Henshall & Kobow, 2015). Epileptogenesis occurs at the molecular level too. Indeed, several signalling pathways are known to be altered during epileptogenic events. Among them, mTOR and BDNF signalling pathways are an example. BDNF–TrkB signalling alters the transcription of $GABA_A$ receptor subunits in granule cells of the hippocampal dentate gyrus, enhancing glutamatergic transmission while impairing the function of inhibitory synapses (Devinsky et al., 2018). Given the pivotal role of the mTOR pathway in cellular functions and neuronal excitability, it is not surprising that this signalling pathway can be involved in the development of spontaneous seizures, representing an important target for both epileptogenesis and seizure pharmacotherapy. Accordingly, hyperactivated mTOR signalling has a main role in the pathogenesis of different animal models of acquired epilepsy and several studies have demonstrated that mTOR inhibitors, such as rapamycin, decrease the development of seizures preventing epileptogenesis-related mechanisms (Citraro et al., 2016). Interestingly, both pathways are involved also in structural changes of aberrant mossy fibre sprouting in the hippocampal granule cell layer, innervating inhibitory basket cells and decreasing neuronal excitability. Degeneration of excitatory mossy cells and the loss of inhibitory GABAergic and

neuropeptidergic hilar interneurons is likely linked to this anomalous sprouting (Devinsky et al., 2018).

One of the main pharmacological treatment against epilepsy are antiepileptic drugs (AEDs). Antiepileptic drugs are currently the main solution for some forms of epilepsy, even though their activity is still limited and mostly active at the level of the excitatory/inhibitory imbalance. They act at different levels: they modulate voltage-gated ion channels, like sodium, calcium and potassium channels, or enhancing inhibitory activity thus reducing the brain hyperexcitation. Given the pivotal role of voltage-gated ion channels in regulating neuronal excitability, some AEDs like phenytoin, carbamazepine and lamotrigine act at this level, limiting neuronal activity triggered by these channels. Others AEDs act through the enhancement of GABAergic inhibition, as barbiturates, benzodiazepine and vigabatrin and tiagabine (Kwan & Brodie, 2006; Mula, 2018).

Unfortunately, not all epilepsy forms are responsive to AEDs treatments. Despite the generation of new compounds every year for treating this disease, epilepsy remains uncontrolled in up to one-third of patients. Indeed, it has been estimated that around 15 million people worldwide have drug-refractory epilepsy (Mula, 2016). The alternatives for these refractory epilepsies can be the surgical removal of the epileptogenic focus, or the stimulation of the vague nerve. Another option is the ketogenic diet, a very restrictive dietary regimen, consisting in high-fat, low-protein a low-carbohydrate diet. The exact mechanism on seizure suppression is still not univocal,

but mimicking a system that recreates the keto-acidotic state seems to have an effect on epilepsy (Kwan & Brodie, 2006).

A recent and promising strategy to treat epilepsy is represented by gene therapy. Through the modification of endogenous genes, by targeting small brain regions without introducing the expression of foreign proteins, it is possible to restore the correct neuronal network activity with an approach that is generally considered as safe (Kullmann et al., 2014). For example, this approach has been used in a mouse model of chronic TLE. By applying the CRISPR/Cas9 toolbox, the endogenous Kcna1 expression has been increased in order to modulate neuronal activity, decreasing seizure initiation and rescuing behavioural and transcriptomic abnormalities. Thus, this promising tool can be used to regulate the expression of different genes, representing the way to treating many possible epilepsy disorders associated with loss-of-function mutations and haploinsufficiency (Colasante et al., 2020).

Indeed, in the last years, thanks to the recent advances in the neurobiology and genetics fields, specific genetic mutation have been found to be related to different forms of epilepsy, including focal epilepsy. In particular, mutations in genes encoding for the mTOR pathway components were found in tuberous sclerosis and other genetic syndromes, focal cortical dysplasia, non-lesional focal epilepsy, as well as post-traumatic epilepsy, making this pathway a potential novel target for epilepsy treatments (Myers & Scheffer, 2017).

2.4 The mTOR pathway and its regulation

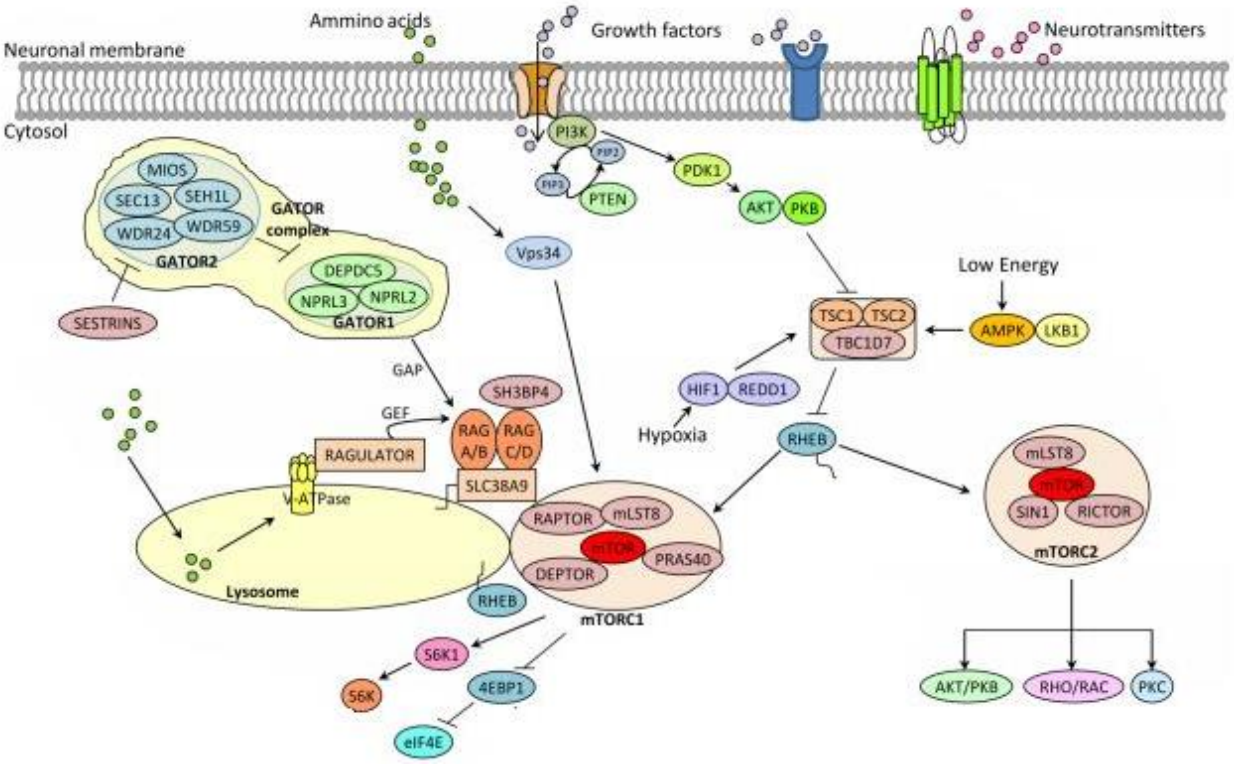

Figure 2. General overview of the mTOR pathway: upstream regulation, the protein complexes involved and downstream effectors (modified from Baldassarri et al., 2016).

Mechanistic (previously known as mammalian) target of rapamycin, mTOR, is a well conserved 289 kDa PI 3-kinase (PIKK) and it is characterized by serine-threonine kinase activity.

Genetic screening in the early '90s identified for the first time TOR in the budding yeast *Saccharomyces cerevisiae*, as the mediator to the inhibitory effect of rapamycin on the growth process. Shortly thereafter, the mammalian ortholog was isolated using FKBP12-rapamycin affinity purification (Bockaert & Marin, 2015; González & Hall, 2017). mTOR

forms two structural and functional distinct complexes named mTOR complex 1 (mTORC1) and mTOR complex 2 (mTORC2), respectively. Both mTOR complexes are large, with mTORC1 having six and mTORC2 seven known protein components. mTORC1 is the best characterized of the two complexes and together with mTORC2 shares the catalytic mTOR subunit, mammalian lethal with sec-13 (mLST8), DEP domain containing mTOR-interacting protein (DEPTOR) and the Tti1/Tel2 complex. Regulatory-associated protein of mammalian target of rapamycin (Raptor) and proline-rich Akt substrate 40kDa (PRAS40) take part specifically in mTORC1, while rapamycin-insensitive companion of mTOR (Rictor), mammalian stress-activated map kinase-interacting protein 1 (mSin1) and protein observed with Rictor 1 and 2 (protor1/2) participate only in mTORC2. (Laplante & Sabatini, 2012) .

The role of mTOR is to sense and integrate diverse intra- and extra-cellular signals to regulate a variety of cellular processes, ranging from cell growth to metabolism and survival, mainly through the regulation of gene and protein expression (Ryther & Wong, 2012). In particular, mTORC1 senses nutrients such as glucose, amino acids, oxygen, ATP and growth factors. All this cues activate a pathway controlling a variety of cellular processes, including protein and lipid synthesis and autophagy (Laplante & Sabatini, 2012).

Compared to mTORC1, the mTORC2 pathway is less defined. mTORC2 is insensitive to nutrients, but it is able to respond to growth factors like insulin and thus controls cell survival, apoptosis, cell proliferation and cell shape. Moreover, since the acute treatment with rapamycin does not alter mTORC2 signaling as it does with m TORC1,

this complex was originally thought to be rapamycin-insensitive. However, long-term treatment with rapamycin reduces mTORC2 signaling in some cell types by suppressing mTORC2 assembly, but this mechanism is far from being clear (Laplante & Sabatini, 2012).

2.4.1 Upstream regulation of mTORC1

The integration of diverse intra- and extra-cellular clues activating mTORC1 allows this protein complex to orchestrate a variety of physiological effects and control major cell processes, including protein and lipid synthesis and autophagy. The generation of a variety of different outcomes is therefore possible by the involvement of various effector pathways.

The majority of the pathways that control both positively and negatively mTORC1 involve the heterodimer consisting of tuberous sclerosis 1 (TSC1; also known as hamartin) and TSC2 (also known as tuberin). TSC1/2 is indeed a key upstream regulator of mTORC1 and exerts its function as a GTPase-activating protein (GAP) for the Ras homolog enriched in brain (Rheb) GTPase. The GTP-bound form of Rheb directly interacts with mTORC1 and strongly stimulates its kinase activity. As Rheb GAP, TSC1/2 negatively regulates mTORC1 by converting Rheb into its inactive GDP-bound form (Laplante & Sabatini, 2012).

The canonical activation of the mTOR pathway by growth factors, such as such as insulin and insulin-like growth factor 1 (IGF1), starts from the activation of tyrosine kinase

receptors (RTKs) that stimulate the PI3K and Ras pathways. The effector kinase of this pathway, Akt, extracellular-signal-regulated kinase 1/2 (ERK1/2), and ribosomal S6 kinase (RSK1) inactivate the heterodimer TSC1/TSC2 by direct phosphorylation and thus result in mTORC1 activation (Bockaert & Marin, 2015; Laplante & Sabatini, 2012).

Similarly to the mechanism of mTORC1 pathway activation by growth factors, pro-inflammatory cytokines, like tumor necrosis factor-α (TNFα), induce phosphorylation of TSC1 by IκB kinase β (IKKβ), causing TSC1/2 inhibition (Laplante & Sabatini, 2012).

Also low energy levels, hypoxia and DNA damage signal to mTORC1 through TSC1/2. In particular, the signaling pathway involves adenosine monophosphate-activated protein kinase (AMPK). AMPK phosphorylates TSC2 and increases its GAP activity towards Rheb and, being in direct contact with mTORC1, phosphorylates Raptor, leading to mTORC1 inhibition.

Low-oxygen levels lead to the expression of transcriptional regulation of DNA damage response 1 (REDD1), which activates TSC2 function through a mechanisms that is not fully understood, while DNA damage also signals to mTORC1 through multiple mechanisms requiring p53-dependent transcription. DNA damage also induces the expression of *Tsc2* and phosphatase and tensin homolog deleted on chromosome 10 (Pten), inducing the downregulation of the PI3K-mTORC1 axis (Bockaert & Marin, 2015; Laplante & Sabatini, 2012).

The TSC1/2 complex is not involved in the amino acid-mediated mTORC1 activation. Indeed, another heterodimer, composed of RagA/B and RagC/D, is needed to induce

mTORC1 translocation from the cytosolic compartment to the lysosome surface, where it can be activated by GTP-Rheb (Laplante & Sabatini, 2012).

Another protein complex involved in the amino acid sensing branch is GATOR1, an upstream inhibitor of mTORC1. It is a GTPase Activating Protein (GAP) for RagA, consisting of Depdc5, NPRL2 and NPRL3 (Shen et al., 2018). GATOR1 activity is inhibited by GATOR2 protein complex, leading to the opposite effect of m TORC1 activation. (Bockaert & Marin, 2015; Shen et al., 2018). Recently, mutations in genes encoding GATOR1's components have been found to be associated with several genetic focal epilepsy (FE) syndromes, including autosomal dominant nocturnal frontal lobe epilepsy (ADNFLE), familial temporal lobe epilepsy (FTLE), dominant epilepsy with auditory features (ADEAF), and familial focal epilepsy with variable foci (FFEVF) (Baldassari et al., 2016).

2.4.2 Downstream effects of mTORC1 activation

Several studies in the last years, including large phosphoproteomic screens, identified new potential targets of mTORC1 (Switon et al., 2017). Protein synthesis is one the process known to be regulated by mTORC1 activity, yet poorly characterized. Given the pivotal role of protein synthesis in cell metabolism, the regulation of this process occurs based on nutrient disposal and general conditions of the cell. mTOR kinase is the main factor that links the energy state of the cell to protein translation. In the canonical pathway, mTORC1 directly interacts and phosphorylates the translational regulators

eukaryotic translation initiation factor 4E (eIF4E) binding protein 1 (4E-BP1) and ribosomal S6 kinase 1 (S6K1). Induction of protein synthesis occurs through inhibition of 4E-BP1 with the subsequent release of inhibition of eIF4E. On the other hand, S6K1 promotes protein synthesis by increasing mRNA biogenesis, as well as translational initiation and elongation by phosphorylating ribosomal protein S6 (Laplante & Sabatini, 2012; Sadowski et al., 2015).

mTORC1 not only promotes protein synthesis, but it is also involved in the synthesis of lipids required to generate membranes for proliferating cells. To do so, mTORC1 acts on the sterol regulatory element binding protein 1/2 (SREBP1/2) transcription factors regulating the expression of numerous genes involved in fatty acid and cholesterol synthesis (Laplante & Sabatini, 2012).

mTORC1 activity negatively controls the initiation of macro-autophagy, and the latter process can be induced either through mTORC1 inhibition with rapamycin or amino acid starvation. mTORC1 inhibits the autophagic process through the inhibition of the ULK1 complex (Unc-51- like kinase 1 [ULK1]–autophagy-related protein 13 [Atg13]–FAK family kinase-interacting protein of 200 kDa [FIP200] complex and autophagy/Beclin-1 regulator 1 [AMBRA]). Another mechanism through which mTORC1 regulates macro-autophagy occurs though the phosphorylation of the transcription factor EB (TFEB), which regulates the expression of some genes involved in autophagosome biogenesis (Bockaert & Marin, 2015; Laplante & Sabatini, 2012; Switon et al., 2017).

Overall, the mTOR pathway plays a key role in the physiological regulation of normal cellular function and processes, while its dysregulation leads to the development of disease under pathological conditions such as type 2 diabetes, inflammation, cancer, and cardiovascular pathologies. Furthermore, alteration of the normal mTOR signaling is involved in a variety of neurological diseases, including epilepsy, psychiatric and neurodegenerative disorders (Citraro et al., 2016). The name 'mTORopathies' collectively indicates a number of clinical syndromes in which mTOR regulation is altered (Griffith & Wong, 2018). Given the wide range of neuronal and non-neuronal functions controlled by the mTOR signaling pathway, it is not surprising that its regulation through pharmacological inhibitors, such as rapamycin and its derivatives, has controversial effects. In the murine genetic TSC model, suppressing mTOR activity using rapamycin administered in prenatal, postnatal and pre/postnatal (combined) temporal windows reduce seizure frequency, neuronal and glial pathology, thus interfering with the epileptogenic process (Way et al., 2012). Surprisingly, the animals treated with the combined therapy do not perform well as postnatally-treated animals in learning and memory tasks, indicating a necessary optimization of the timing and dosage of the rapamycin treatment (Way et al., 2012). On the other hand, a phase III clinical trial demonstrated that a rapamycin-derived compound, Everolimus, exhibited anti-seizure activity in a cohort of patients affected by TSC (French et al., 2016). Moreover, limitation of mTOR activity also affects growth and proliferation, protein and lipid synthesis, cell cycle and autophagy, all processes that are necessary for correct physiology and survival of cells. Thus, the efficacy of rapamycin and its pharmacological derivatives in both

animal models and patients is still debatable and the precise mechanism of action underlying their therapeutic effects could by influenced by the animal model and the specific etiology (Devinsky et al., 2018).

2.4.3 The specific role of mTORC1 in the brain

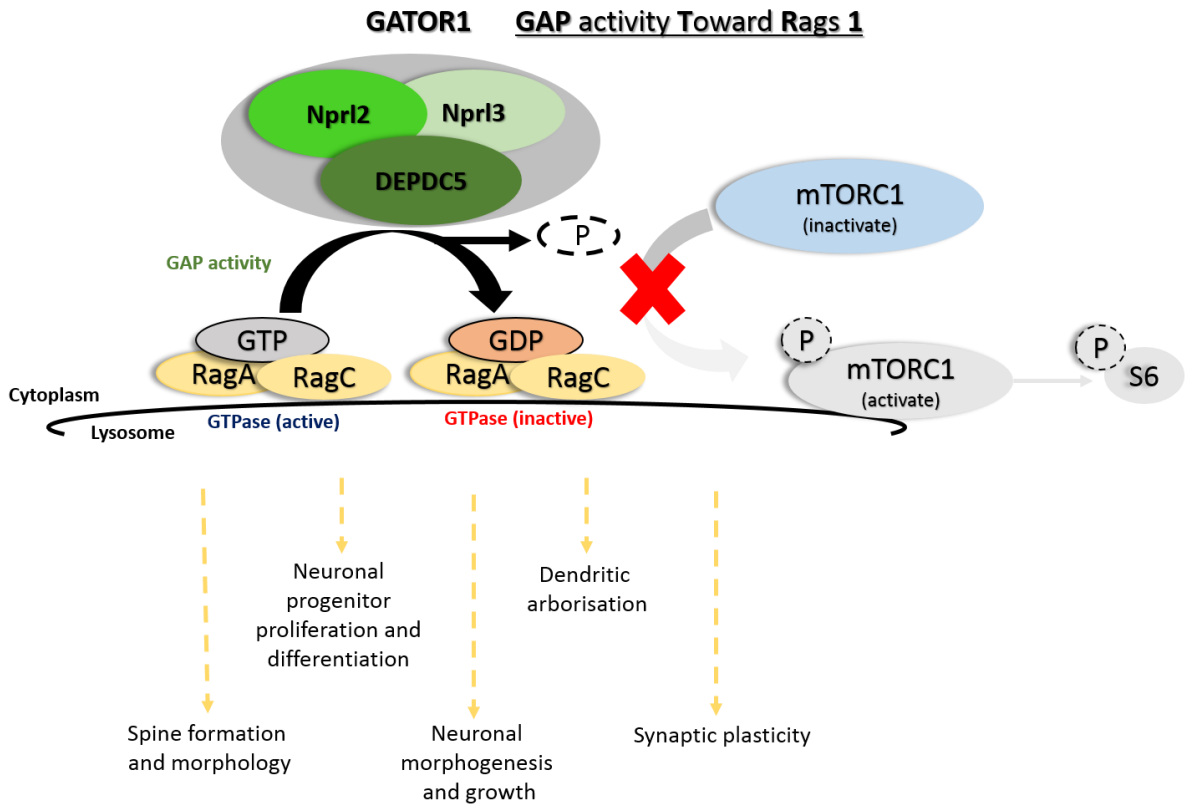

Figure 3. Different roles of mTORC1 in the brain and its regulation by GATOR1 complex (modified from Baulac, 2014).

Given the pivotal role of mTORC1 in regulating numerous cellular processes, it is not surprising that it plays a major role also in controlling brain physiology and pathology. Besides its implication in autophagy, cell size, survival, migration and proliferation, it is a main regulator of some more specific neuronal processes, such as axonal sprouting and regeneration, myelination, dendritic spine growth and ionic channels and neurotransmitter receptor expression. mTORC1 activity is able to regulate higher

physiological functions such as neuronal excitability, neuronal survival, synaptic plasticity and cognition; therefore, mutations of genes coding for proteins involved in the mTOR pathway, or alteration in their expression level, could underlie different brain diseases. Some of these are psychiatric diseases such as depression, mental retardation, schizophrenia, Down syndrome, and autism spectrum disorders (ASD), including tuberous sclerosis (TSC), Fragile X, neurofibromatosis, and Rett syndrome. Alteration of mTOR has also been involved in neurological diseases, particularly in different forms of epilepsies, Parkinson's disease (PD), Alzheimer's disease (AD), and brain trauma (Bockaert & Marin, 2015).

2.4.3.1 Neuronal progenitor proliferation and differentiation

The central role of mTOR in neuronal differentiation is well established. Indeed, PI3-kinase/TOR signaling during neurogenesis in the developing mouse and chick is necessary for the correct neuronal development. Mice lacking PDK1/PKB activity and chick neural tube exposed to PI3-kinase or TOR inhibitors showed disrupted neurogenesis (Fishwick et al., 2010). Deletion of the upstream inhibitor of mTORC1, REDD1, induced cell cycle exit impairing neuronal differentiation and migration (Malagelada et al., 2011), while deletion of PTEN, inhibitor of the Akt-mTORC1 pathway, triggers constitutive neurogenesis in the subventricular zone (SVZ) neurogenic niche in the adult brain (Gregorian et al., 2009). Moreover, it has been demonstrated the key role of enhancer of zest homolog2 (Ezh2) in the regulation of PTEN-Akt-mTOR pathway

in SGZ, is essential not only for hippocampal neurogenesis, but also for preserving cognitive functions (Zhang et al., 2014).

2.4.1.2 Neuronal morphogenesis and growth

Neuronal hypertrophy if a characteristic of most brain pathologies in which an hyperactivation of mTORC1 is present, such as in Tuberos Sclerosis (TS) with mutations in *TSC1* or *TSC2*, Fragile X syndrome (mutations in *FMRP*) or Cowden syndrome (mutations in *PTEN*), hemimegalencephaly and ganglioglioma (Bockaert & Marin, 2015). Hypertrophic cells have a soma 1.5-2 times larger than normal cells and have been found in cortex, hippocampus and cerebellum. Rapamycin administration revertes the phenotype, confirming the mTORC1 hyperactivation-dependence of this process. In human mTORopathies, this effect is especially evident in patients affect by TSC, displaying giant cells within the tuber (Lasarge & Danzer, 2014), or in patient suffering from Focal Cortical Dysplasia (FCD), a condition characterized by the presence of the so called “balloon cells”.

Alteration in cell shape and size leads to several consequences both at the micro- and macroscopic level. Indeed, at the single cell level, an increased soma area decreases the cell input resistance and increases the total cell capacitance, while at the macroscopic level, hypertrophy can lead to increased brain size and loss of organization of the cortical layers (Lasarge & Danzer, 2014).

2.4.1.3 Dendritic arborisation, synaptic physiology and plasticity processes

The structure of the dendritic tree is essential for precise signal processing. Indeed, changes in dendritic thickness induced by mTOR dysregulation can potentially lead to an altered synaptic input integration (Lasarge & Danzer, 2014). It has been demonstrated that the dendritic growth and branching process is regulated through PI3K/PTEN–mTOR pathway and that the silencing of PTEN triggers an increase in the number and total length of dendrites, and an increase in branching complexity (Jaworski et al., 2005).

mTORC1 activation is also involved in the regulation of ion channel expression. It has been shown that, upon m TORC1 activation, NMDA receptor activation occurs and, in turn, inhibits local Kv1.1 synthesis, likely via PI3K activation by Ca^{2+} entry, thus facilitating action potential generation (Raab-Graham, Haddick, Jan, & Jan, 2006). mTORC1 is also involved in surface expression of AMPA receptors (AMPARs) in cortical neurons, enhancing synaptic activity. Indeed, a rapamycin-sensitive increase in the expression of AMPARs subunits GluR2/3 has been observed in primary cortical neurons (Wang, Barbaro, & Baraban, 2006). On the opposite, in hypothalamic pro-opiomelanocortin (POMC) neurons, an increase of total K_{ATP} channel conductance is triggered by the age-dependent increase in mTORC1 activity, thus silencing the activity of POMC neurons and contributing to age-dependent obesity (Yang et al., 2012). Given its role in the regulation of protein expression, a fundamental process occurring during long-term plasticity, it is not surprising that mTORC1 acts as a regulator in this mechanism too, as shown in different organisms such as Aplysia, crayfish, and mammals. In particular, late-stage Long Term Potentiation (L-LTP), in which transcription and

translocation of new proteins is needed, is a cAMP- and mTORC1-dependent process (Cammalleri et al., 2003). cAMP synthesis could lead to m TORC1 activation by inducing Ca^{2+} entry from NMDAR and activation of Ca^{2+}-dependent adenylyl cyclase. On the other hand, cAMP production triggers BDNF release, that in turn activates the PI3K-Akt-mTOR pathway (Bockaert & Marin, 2015). However, some contradictory data exist, according to which administration of rapamycin does not block L-LTP in thedentate gyrus in vivo and the lack of S6K1 or S6K2 does not affect normal L-LTP in mice (Bockaert & Marin, 2015).

2.5 GATOR1 complex and its key role in Focal Epilepsy

Recent studies revealed that Focal Epilepsy (FE) accounts for more than the half of the total cases of all epileptic syndromes, around 60%. It can be caused by both genetic and acquired factors, but in most cases it has a genetic basis (Baldassari et al., 2016; Boillot & Baulac, 2016; Téllez-Zenteno & Hernández-Ronquillo, 2012). Familial Focal Epilepsies (FFEs) include several forms of inherited autosomal dominant, non-lesional, focal epilepsies. These can be distinguished into autosomal dominant nocturnal frontal lobe epilepsy (ADNFLE), familial temporal lobe epilepsy (FTLE), dominant epilepsy with auditory features (ADEAF), and familial focal epilepsy with variable foci (FFEVF).

The results of earlier genetic studies for ADNFLE, a syndrome characterized by clusters of motor seizures occurring mostly during sleep, revealed a correlation between mutation in genes encoding for ion channels and neurotransmitter receptors. Indeed, in 1995, the first mutated gene related to an inherited form of focal epilepsy, ADNFLE, was identified (Steinlein et al., 1995). The gene was CHRNA4, encoding for a subunit of the nicotinic acetylcholine receptor (nAChR). Later studies identified mutations in other nAChRs subunits, CHRNB2 and CHRNA2 already related to a subset of ADNFLE (Boillot & Baulac, 2016). More recently, mutations in the potassium channel KCNT1 gene have been found to associate with ADNFLE. The first mutation in a gene other than ion channels or neurotransmitter receptors is LGI1, which was identified in families with ADEAF, a syndrome presenting focal seizures with typical auras and/or auditory

symptoms suggesting a lateral temporal onset. Mutations in this gene account for almost 50% of ADEAFs (Ottman et al., 2004).

Only recent studies discovered the link between diverse focal epileptic phenotypes, ranging from apparently non-lesional focal epilepsies to malformation-associated focal epileptic syndromes with mutation in genes encoding for components involved in the regulation of the mTOR pathway, especially the components of the GATOR1 complex, Depdc5, NPRL2/3 (Baldassari et al., 2019).

In 2013, mutations in Depdc5 gene were first identified in seven out of eight FFEVF families linked to chromosome 22q12. This mutations were found to be implicated in the 5%–37% of a broad range of FEs, including NFLE and TLE (Dibbens et al., 2013; Ishida et al., 2013). Few years later, in 2016, mutations in NPRL2 and NPRL3 were found in patients with FE, confirming the key role of the entire GATOR1 complex in the pathogenesis of FE syndromes (Ricos et al., 2016; Sim et al., 2016). More recently, a bialellic 2-hit mutational mechanism, with brain somatic and germline mutations of the *DEPDC5* gene, was observed in resected brain tissue of patients with the most severe symptomatology, including focal cortical dysplasia type II (FCD type II; Ribierre et al., 2018). To demonstrate the causality of this *DEPDC5* brain mosaic inactivation, they performed *in utero* electroporation using CRISPR-Cas9 editing in mice, generating an animal model that finally recapitulated FE with cortical malformation and severe phenotype, indicating that loss of heterozygosity is necessary for the establishment of epilepsy-associated FCD observed in patients (Ribierre et al., 2018).

Overall, these data indicate that mutations in genes encoding the GATOR1 complex can be defined as the most frequent genetic cause of FEs, globally underlying the 9% of the cases. This finding suggests the possibility that defects in the same molecular pathway can lead to the development of different form of focal epilepsy (Baldassari et al., 2016).

2.6 The *DEPDC5* gene: role and function

DEPDC5 gene is located on chromosome 22q12 and encodes the 1603–amino acid protein Disheveled, Egl-10, and Pleckstrin (DEP) domain-containing 5 (DEPDC5). The protein presents five domains, N-terminal domain (NTD), SABA (previously annotated as DUF3608, Domain of Unknown Function 3608), SHEN, DEP and the C-terminal domain (CTD) that have been resolved and visualized for the first time only recently (Shen et al., 2018). It is the largest subunit of the GAP Activity Toward Rags complex 1 (GATOR1), an inhibitor of the mTORC1 pathway, together with NPRL2 and 3.

DEPDC5 is connected to NPRL3 by NPRL2, which in vitro acts as a GTPase-activating protein (GAP) for Rag GTPases, in particular Rag A/B. The interaction between DEPDC5 and the Rag heterodimer blocks the GATOR1 ability to stimulate GTP hydrolysis, while NPRL2-NPRL3 and RagA interaction executes the GAP activity. Rag GTPases are present in heterodimers of RagA or RagB, which are highly homologous with either RagC or RagD. Their function is to mediate amino acid signaling to mTORC1 and the amino acid-induced re-localization of mTOR within the endomembrane system of the cell (Bar-Peled et al., 2013; Sancak et al., 2008). Components of both GATOR complexes are highly conserved across evolution and have been well characterized in yeast *S. cerevisiae* (Algret et al., 2014; Dokudovskaya & Rout, 2015). In yeast, the DEPDC5 orthologous protein Sea1 (also known as Iml1) is part of the SEA complex with Npr2 and Npr3, and functions as a GAP complex to inhibit the Rag-dependent activation of TORC1 (Panchaud et al., 2013).

The recent discovery of an association between mutations in *Depdc5* gene with a broad range of FEs make *Depdc5* a promising and potential therapeutic target for epilepsy treatment (Baldassari et al., 2016; Dibbens et al., 2013; Ishida et al., 2013; Myers & Scheffer, 2017).

2.7 Models of *DEPDC5* deficiency

Given the major involvement in *DEPDC5* gene and related mutations in FEs, an increasing number of studies focused their attention in characterizing *DEPDC5* loss-of-function models. In 2016, Marsan and colleagues investigated the effect of *in vivo Depdc5* loss in rat. By using TALEN-mediated *Depdc5* knock out rat, they demonstrated that constitutive deletion of *Depdc5* is embryonically lethal, while the heterozygous rats develop normally in the absence of spontaneous electroclinical seizures, but presenting cortical neuron excitability and firing patterns (Marsan et al., 2016). The *in vivo* effect of *Depdc5* deficiency was further investigated by Hughes and colleagues in 2017, generating mice with loss-of-function alleles using CRISPR/Cas9 mutagenesis. Their experiments were in line with the previous evidence by Marsan*: Depdc5* null mice showed embryonal death, growth defects in different organs and systems and mTORC1 hyperactivation in embryonic brain lysates (Hughes et al., 2017). In order to overcome the problem of embryonic lethality in germline knockout *Depdc5* rodent model, a neuron-specific *Depdc5* cKO mouse by Cre-recombination under the *Synapsin1* promotor (*Depdc5*cc+) was developed. These mice actually survive to adulthood, but with a reduced survival compared to control littermates. They present morphological malformations in the form of larger brains with increased and dysplastic cortical neurons size, hyperactivation of the mTORC1 pathway and increased susceptibility to both spontaneous and provoked seizure (Yuskaitis et al., 2018). Moreover, the chronic inhibition of the mTORC1 pathway with rapamycin seems to significantly prolong the

survival of *Depdc5*cc+ mice, by rescuing the morphological abnormalities and mTORC1 hyperactivation (Yuskaitis et al., 2019). *Depdc5* loss-of-function has also been studied in lower animal models, such as Zebrafish. By a morpholino oligonucleotide-mediated *Depdc5* knockdown, authors showed an increase in neuronal activity (de Calbiac et al., 2018), while in another work, a zebrafish full knockout model showed increased seizure propensity, premature death and defects in the GABAergic system (Swaminathan et al., 2018). Alteration of the GABAergic system have also been found in a novel mouse model of Depdc5 deficiency generated by conditional deletion of *Depdc5* in dorsal telencephalic neuroprogenitor cells. These neurons, apart from showing enlarged soma size and mTORC1 hyperactivity, also present impaired postsynaptic responses to GABAergic inputs, which may generate hyperexcitability and represent the epileptogenic mechanism (Klofas et al., 2020).

Recently, it has been proposed that a “two-hit” mosaic inactivation, brain somatic and germline, of the DEPDC5 gene is present in patients with the most severe phenotypes. To demonstrate this hypothesis, Ribierre and colleagues induced *Depdc5* brain mosaic inactivation using CRISPR-Cas9 editing and in utero electroporation in the mouse cortex, recapitulating focal epilepsy with FCD and SUDEP-like events (Ribierre et al., 2018). All these experimental models were able to reproduce some of the main clinical features of DEPDC5-related epilepsy; however, the mechanisms underlying the morphological and physiological effect of DEPDC5 deficiency on synaptic transmission, plasticity and connectivity are still to be clarified.

In this contest, we decided to further investigate the mechanisms by which *DEPDC5* loss-of-function triggers neuronal and network hyperexcitability. In our first study published at the beginning of the 2020, we investigated the cellular mechanisms of hyperexcitability by comparing the constitutively heterozygous Depdc5 knockout mouse *versus* various levels of acute Depdc5 deletion (≈40% and ≈80% neuronal knockdown of Depdc5 protein) by RNA interference in primary cortical cultures. While heterozygous *Depdc5*$^{+/-}$ neurons show a weaker phenotype, acutely knocked-down neurons exhibit a strong dose-dependent phenotype, showing mTOR hyperactivation accompanied by increased soma size, dendritic arborization, excitatory synaptic transmission and intrinsic excitability. These results highlights the importance of the temporal dynamics of Depdc5 knockdown in triggering the phenotypic changes, reminiscent of the somatic second-hit mechanism in patients with focal cortical dysplasia and suggesting the importance of DEPDC5 in the developmental process. Moreover, we observed synaptic alterations only at the level of excitatory synapses, with no effect on the inhibitory synapses. These evidences, strengthen the hypothesis of an excitation/inhibition imbalance triggering epileptogenesis and the pivotal role of DEPDC5 in neurodevelopment (De Fusco*, Cerullo* et al., 2020).

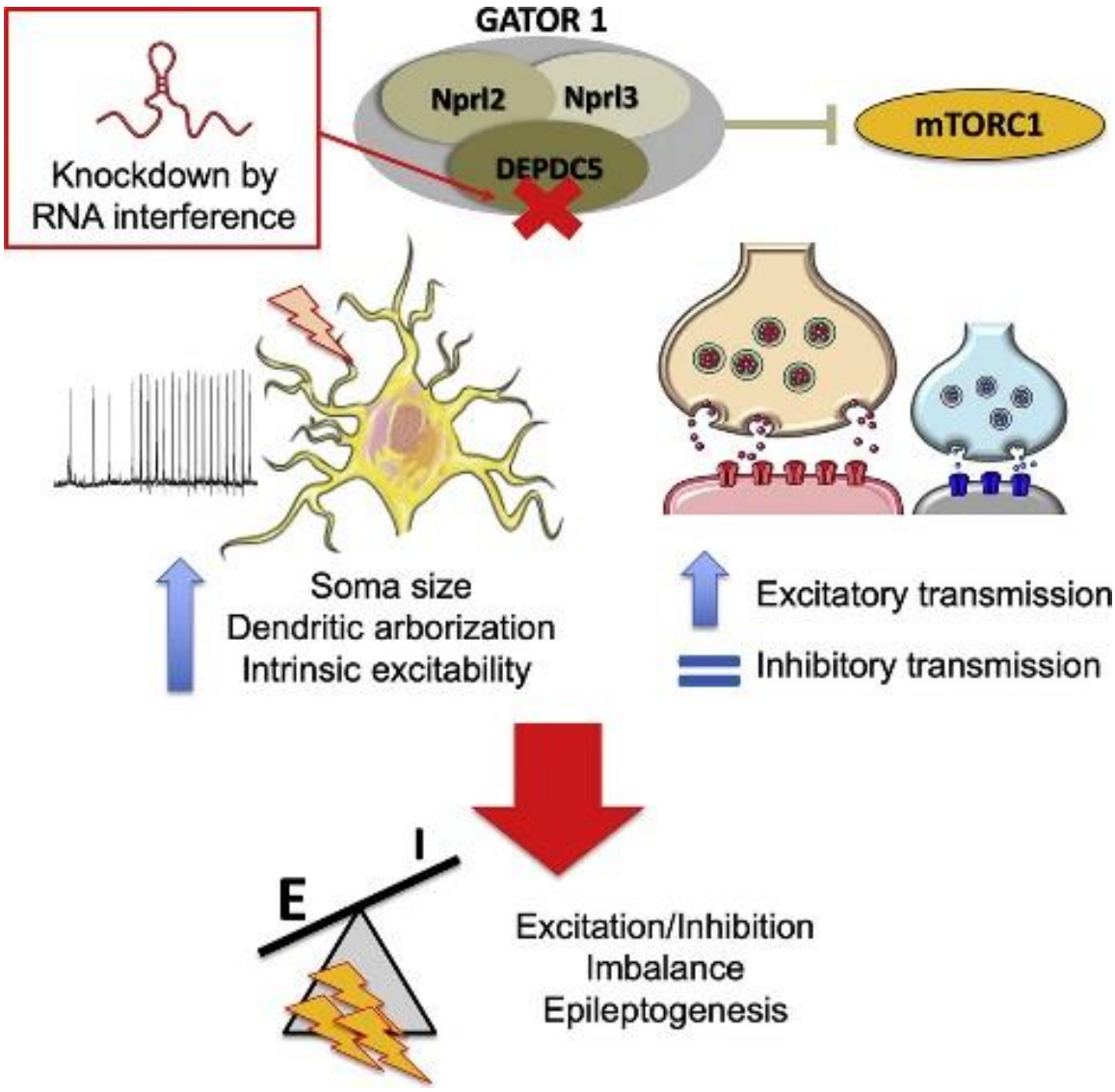

Figure 4. Acute Depdc5 knockdown leads to a robust neuronal and synaptic phenotype. It increases neuronal soma size and dendritic arborizations, alters synaptic connectivity and induces an excitation/inhibition imbalance at the synaptic level. The hyperexcitability of excitatory neurons further increases excitatory strength (from De Fusco*, Cerullo* et al., 2020).

3. Aim of the thesis

The aim of this PhD project is to deepen the pathological role of *Depdc5* loss on synaptic transmission and plasticity. In order to address this issue, we applied the Cre/LoxP technique, characterizing the effect of *Depdc5* conditional knockout by performing electrophysiological and biochemical experiments on primary cortical neurons obtained from *Depdc5*-floxed pups. By transfecting cortical neurons with lentivirus expressing active or inactive Cre recombinases, we observed the effect of Depdc5 cKO at the level of both excitatory and inhibitory synapses, analyzing synaptic transmission and short-term plasticity processes. Our data suggest that the *Depdc5* loss mostly induces a change at the level of synaptic connectivity, by increasing the number of excitatory synapses and enhancing excitatory synaptic transmission with a predominant action at the postsynaptic level.

4. Materials and Methods

Animal models

Dedpc5-floxed mice were kindly donated from Stephanie Baulac Lab (Paris Brain Institute - Institut du Cerveau – ICM) and bred at the IIT-San Martino animal facility. To detect homozygous *Depdc5*-floxed mice, genotyping was performed by PCR with the following primers Depdc5_F: AGCAAGATGACTTCCCTGCTCCAAGA, Depdc5_R: CTGTGCTCTCATTTCCAACCATCCCT. The colony was maintained and propagated in homozygosity. Constitutive heterozygous Depdc5 KO mice were obtained from the IMPC European Consortium at the Sanger Institute (UK) and bred at the IIT animal facility. EUCOMM/KOMP targeting strategy was based in the “knockout-first” allele (Tm1a) designed to be a knockout by splicing the cDNA to a LacZ cassette, which was inserted into the intronic region, between exons 4 and 5 of *Depdc5* locus, creating a null allele of the gene (Skarnes et al., 2011). Genotyping was performed by PCR with the following primers Depdc5_F: GGTTTTAGTTTTTGGATTTGTTTCA, Depdc5_R: GCCTTTAATCCCAGCACTTG; 5mut-R1_Term: GAACTTCGGAATAGGAACTTCG, that were used to detect the WT (+/+) (Depdc5_F plus Depdc5_R product, 227 bp) and mutant (Depdc5_F plus CAS_R1_Termproduct, 129 bp) Depdc5 alleles and to genotype wild type (+/+) and heterozygous (+/−) mice. The colony was maintained and propagated in heterozygosity. Both *Dedpc5*-floxed mice and constitutive heterozygous Depdc5 KO mice were maintained on a 12:12 h light/dark cycle at a constant temperature (21 C°)

and relative humidity (60%). Drinking water and a complete pellet diet (Mucedola, Settimo Milanese, Italy) were provided to mice ad libitum. Two females were housed with one male in standard Plexiglass cages (33 x 13 cm), with sawdust bedding and metal top. After two days of mating, male mice were removed and dams were housed individually and daily checked for delivery. All the experiments were carried out in accordance with the guidelines established by the European Communities Council (Directive 2010/63/EU of March 4th, 2014) and were approved by the local Ethics Committee and the Italian Ministry of Health.

Low-density and autaptic cultures of cortical neurons

Low-density primary cortical neurons were obtained from postnatal *Depdc5*-floxed mice (P0-1), as previously described (Beaudoin et al., 2012; Valente et al., 2016). In brief, cortices were dissociated by enzymatic digestion in 0.25% trypsin for 6 min at 37 °C and mechanically triturated with a pipette and plated the desired density. For cell culture preparations, the following solutions were used: HANKS solution, prepared from HBSS (GIBCO 14170-088; red) supplemented with 10 mM HEPES, 30 mM D-glucose, 5 µg/ml Gentamycin, pH 7.4 with KOH; dissection solution, prepared from HANKS solution supplemented with 10% bovine serum albumin and 6 mM $MgSO_4$*$7H_2O$. Primary cortical neurons were plated at low density (100 cells/mm^2) on 3.5-cm-diameter Petri dishes (Falcon® 35 mm) treated for 24 h with poly-L-lysine (0.1 mg/ml; Sigma-Aldrich) in borate buffer (0.1 M). For autaptic neurons, cells were plated at very low density (20 cells/mm^2)

on microislands (40–300 μm diameter) obtained by spraying of poly-L-lysine (0.1 mg/mL) in buffer borate (0.1 M) on Petri dishes pre-treated with 0.15% agarose, as previously described (Chiappalone et al., 2009; Valente et al., 2012). Cells were grown in a culture medium consisting of Neurobasal A (Gibco™) supplemented with 2% B-27 (Invitrogen, Italy), 1 mM Glutamax, and 5 μg/ml Gentamycin and maintained at 37 °C in a humidified incubator with 5% CO_2.

RNA extraction, retrotranscription and qRT-PCR

Total cellular RNA was extract with TRIzol (Life Technologies) and RNA concentration was quantified by using the Nanodrop-1000 spectrophotomer (Thermo Scientific). cDNA was synthesized starting from 0.25 ug RNA with SuperScript IV Reverse Transcriptase kit (#180900010; Thermo Fisher) according to manufacturer's instruction and used for qRT-PCR. Gene expression was measured by quantitative real-time PCR using C1000 Touch Thermal Cycler (Bio-Rad) on a CFX96 Real time System following the manufacturer's protocol. Real time qPCR analyses were perfomed using the SYBR Green I Master Mix (Roche), on a Lightercycler 480 (Roche), with the following protocol: 95 °C for 5 min; 10 s at 95 °C/ 20 s at the specific annealing temperature (Ta) / 10 s at 72 °C for 45 cycles; melting curve (heating ramp from 55 °C to 95 °C) in order to check for amplification specificity. The following primers (final concentration 0.25 µM) and annealing were used:

*Depdc5*_F: TGATGCCTACGATGCTCAAG, Ta= 64 °C;

*Depdc5*_R: TGGCTCCTCACTTCCTCAGT, Ta= 64.1 °C;

*Gapdh*_F: GATCATCAGCAATGCCTCCT, Ta= 59.8 °C;

*Gapdh*_R: TGTGGTCATGAGTCCTTCCA, Ta= 61.7 °C;

Relative gene expression was determined using the ΔΔCT method, normalizing data and the housekeeping transcript (*Gadph*).

Virus production and neuron transduction

Sequences containing active or inactive Cre-recombinase were cloned into pLenti-PGK-Cre-EGFP or pLenti-PGK-ΔCre-EGFP plasmids (Jaudon et al., 2020; Kaeser et al., 2011). The production of VSV-pseudo typed third-generation lentiviruses was performed as previously described (De Palma and Naldini, 2002). For all the experiments, 6 to 7 days in vitro (DIV) cortical neurons were infected at 10 multiplicity of infection (MOI). After 24 hours from infection, half of the medium was replaced with fresh medium. Transduction efficiency was assessed by visual evaluation of GFP fluorescence. For rescue experiments, rapamycin (100 nM, LC Laboratories) and DMSO (Sigma-Aldrich) as control, were administered at the time of infection, without replacing the medium.

Western blotting

Whole brain from E12.4 mouse embryos or primary cortical neurons were used to obtain total cell lysates. Lysis buffer (150 mM NaCl, 50 mM Tris-HCl pH 7.4, 1 mM EDTA, 1% Triton X-100) enriched with protease and phosphatase inhibitor cocktails (Roche, Monza, Italy) was used to extract cells. Following 10 min of incubation on ice, cell lysates were collected and clarified by centrifugation for 10 min at 10,000 x g at 4 °C. Brains were dissected and pottered in liquid nitrogen, followed by a centrifugation at 1,000 x g for 10 min at 4 °C. To determine protein concentration, the BCA assay (Thermo Scientific) was used. Equivalent amount of proteins were subjected to SDS-PAGE on 10%

polyacrylamide gels and blotted onto nitrocellulose membranes (Whatman). Blotted membranes were blocked for 1 h using 5% milk in Tris-buffered saline (10 mM Tris, 150 mM NaCl, pH 8.0) together with 0.1% Triton X-100 and incubated overnight at 4 °C with the following primary antibodies: rabbit anti-Depdc5 (1:1000, Abcam ab185565), rabbit anti-phosphorylated S6 protein (1:2000, Cell Signaling #5364), mouse anti-S6 (1:1000, Cell Signaling #2317) and mouse anti-actin (1:2000, Sigma-Aldrich A2228). Thereafter, membranes were washed and incubated for 1 h at room temperature (RT) with peroxidase-conjugated goat anti-mouse (1:3000; Bio-Rad) or anti-rabbit (1:5000; Bio-Rad) antibodies. Bands were revealed with the ECL chemiluminescence detection system (Thermo Scientific) and the quantification of immunoreactivity was performed by densitometric analysis of the fluorograms.

Patch-clamp recordings

Whole patch-clamp were made from primary cortical neurons as previously described using a Multiclamp 700B/Digidata 1400A system (Molecular Devices, Sunnyvale, CA). Patch pipettes, prepared from borosilicate glass, were pulled and fire-polished to a final resistance of 4-5 MΩ when filled with standard internal solution. For all the experiments, neurons were maintained in standard extracellular Tyrode solution containing (in mM): 140 NaCl, 2 $CaCl_2$, 1 $MgCl_2$, 4 KCl, 10 glucose, and 10 HEPES (pH 7.3 with NaOH). For the analysis of neuronal excitability, D-(-)-2-amino-5-phosphopentanoic acid (D-AP5; 50 µM), 6-cyano-7 nitroquinoxaline-2,3-dione (CNQX; 10 µM), bicuculline

methiodide (30 μM), and (2S)-3-[[(1S)-1-(3,4-dichlorophenyl)ethyl]amino-2-hydroxypropyl] (phenylmethyl)phosphinic acid hydrochloride (CGP58845; 5 μM) were added to block NMDA, non-NMDA, $GABA_A$, and $GABA_B$ receptors, respectively. Current-clamp recordings of action potential (AP) firing activity were performed at a holding potential of -70 mV and APs were induced by injection of 10 pA current steps lasting 500 ms in morphologically identified pyramidal neurons. Excitatory neurons were identified by estimating the AP failure ratio evoked by short trains of high current steps at increasing frequency (Prestigio et al., 2019). The firing rate was calculated as the number of APs evoked by minimal current injection in 500 ms, whereas the instantaneous frequency was estimated as the reciprocal value of the time difference between the first two evoked APs. Current-clamp recordings of APs were acquired at 50 kHz and filtered at 1/5 of the acquisition rate with a low-pass Bessel filter. The number of elicited APs and the instantaneous frequency were analyzed using Clampfit 10.7 (Molecular Devices, Sunnyvale, CA) and Prism softwares. The shape properties of the first AP elicited by minimal current injection were analyzed by building time-derivatives of voltage (dV/dt) *versus* voltage plots (phase-plane plots), as previously described (Prestigio et al., 2019; Valente, Castroflorio, et al., 2016). Phase-plane plots were obtained and analyzed with the software OriginPro-8 (OriginLab Corp., Northhampton, MA, USA). For recording miniature excitatory postsynaptic currents (mEPSCs), bicuculline, CGP58845, D-APV, and tetrodotoxin (TTX; 300 nM) were added to the extracellular solution to block $GABA_A$, $GABA_B$, NMDA receptors and generation and propagation of spontaneous APs, while for recording miniature inhibitory postsynaptic currents (mIPSCs) bicuculline was replaced

with CNQX. The internal solution (K-gluconate) used for recording APs in current-clamp and mEPSCs in voltage-clamp configuration contained (in mM): 126 K gluconate, 4 NaCl, 1 $MgSO_4$, 0.02 $CaCl_2$, 0.1 BAPTA, 15 glucose, 5 HEPES, 3 ATP and 0.1 GTP (pH 7.3 with KOH). The internal solution (KCl) used for mIPSC recordings contained in (mM): 126 KCl, 4 NaCl, 1 $MgSO_4$, 0.02 $CaCl_2$, 0.1 BAPTA, 15 glucose. 5 HEPES, 3 ATP and 0.1 GTP (pH 7.3 with KOH). All reagents were from Tocris, otherwise specified. Both mEPSCs and mIPSCs were acquired at a 10 kHz sample frequency and filtered at 1/5 of the acquisition rate with a low-pass Bessel filter. The amplitude and frequency of the miniature excitatory and inhibitory events were calculated using a peak detector function using appropriate threshold amplitudes and areas. The frequency, amplitude and kinetics of miniature PSCs were analyzed using the MiniAnalysis (Synaptosoft) and Prism (GraphPad Software, Inc.) softwares. All experiments were performed at RT. Evoked excitatory and inhibitory postsynaptic currents (eEPSCs/eIPSCs) were recorded in Tyrode, with addition bicuculline, D-APV for eEPSCs and D-AP5, CNQX and CGP58845 for eIPSCs. Recordings were performed using an EPC-10 amplifier (HEKA Electronic) and acquired at 10-20 kHz sample frequency and filtered at 1/5 of the acquisition rate with an 8-pole low-pass Bessel filter. The size of the readily releasable pool (RRP) and the probability release (Pr) were calculated using the cumulative amplitude analysis (Schneggenburger, Meyer, & Neher, 1999). RRP was determined by summing up peak PSC amplitudes during 40 repetitive stimuli applied at 40 Hz (1s@40Hz). The cumulative amplitude profiles of the last 15–20 data points were fitted by linear regression and backextrapolated to time 0. The intercept with the Y-axis gave the RRP and the ratio between the amplitude of the

first ePSC (I1) and RRP yielded the Pr. To study the response to paired-pulse protocols, we applied two consecutive stimuli at increasing interpulse intervals (20-1000 ms). Data acquisition was performed using PatchMaster programs (HEKA Elektronic).

Immunocytochemistry

To fix primary cortical neurons, 4% formaldehyde, prepared from paraformaldehyde in 0.1 M phosphate buffer (PB) at a pH 7.4, was used for 20 min at RT. Fixed neurons were immunostained for specific pre/postsynaptic markers of excitatory and inhibitory synapses. Briefly, several washes in PBS, cells were permeabilized and blocked for 30 min in 0.05% Triton X-100 and 10% normal goat serum (NGS) in phosphate buffered saline (PBS) and then incubated overnight with primary antibodies diluted in 3% normal goat serum (NGS) and 0.05% Triton X-100 in PBS. The antibodies were the following: mouse anti-S6 protein (Cell Signaling, #2317), rabbit anti-phosphorylated-S6 protein (Cell Signaling, #2215), guinea pig anti-vGlut1 (1:500, Synaptic System, 135 304), mouse anti-Homer1 (1:200; Synaptic System, 160 011), rabbit anti-vGAT (1:500; Synaptic System 131 003), mouse anti-Gephryn (1:500; 147 011), rabbit anti-GluA1 (1:500; Synaptic Systems, 182 003), rabbit anti-$GABA_A$-β2 receptor subunit (1:500; Synaptic System, 224 803). After three washes in PBS, neurons were incubated in the same buffer with Alexa-conjugated secondary antibodies (1:1500, Invitrogen) and counterstained with Hoechst33342 for nuclei detection. Following several washes in PBS, coverslips were mounted with Moviol mounting medium. Images were acquired using a 40x

objective with a Leica SP8 confocal microscopy (Leica Microsystem, Wetzlar, Germany) and the colocalization plugin of ImageJ was used to process images. To perform the analysis of synaptic density, basal dendrites of neurons were considered, and the colocalization analysis was performed, after threshold subtraction, at the puncta that were double-positive for pre- and post-synaptic markers (vGlut1/Homer1 for excitatory synapses and vGAT/Gephryn for inhibitory synapses). Only GFP-positive neurons were analyzed for experiments with transduced neurons. To identify *bona fide* synaptic boutons, we selected colocalized puncta within an area of 0.1-1 μm^2, corresponding to the overlapping area of pre-synaptic and post-synaptic proteins. The number of synaptic puncta present along 30 μm dendrite tracts starting from the cell body was counted. For the analysis of postsynaptic receptors, the threshold signal of Homer1 and Gephyrin was overlapped to GluA1 and $GABA_A$-β2 receptors, respectively, and the fluorescence intensity was measured only within the colocalization area. Data refer to three independent experiments carried out in duplicate with 5-10 neurons analyzed per duplicate.

Statistical analysis

Data are expressed as means ± SEM or as box plots showing median, mean, 25 to 75 interquartile range and min to max values for number of cells (N) or independent preparations, as detailed in the figure legends. Normal distribution of data was assessed using the D'Agostino-Pearson's normality test ($n>6$) or the Shapiro-Wilk test ($n<6$). The F-test was used to compare variance between two sample groups. To compare two experimental groups, either the two-tailed unpaired Student's *t*-test or the non-parametric Mann-Whitney's *U*-test was used based on data distribution. To compare more than two normally distributed experimental groups, one-way ANOVA (followed by the Bonferroni's multiple comparison test) or repeated measures ANOVA was used. To compare more than two non-normally distributed experimental groups, the Kruskal-Wallis ANOVA was used, followed by the Dunn's multiple comparison test. Significance level was preset to $p<0.05$. Statistical analysis was carried out using Prism (GraphPad Software, Inc., La Jolla, CA).

5. Results

5.1 Characterization of the constitutive *Depdc5* knockdown model

As previously described, *Depdc5* homozygous knockout is embryonically lethal, with prenatal death occurring between E14.5 and E17.5 (Hughes et al., 2017; Marsan et al., 2016). In line with this observation, when mating heterozygous to heterozygous carriers, we never observed *Depdc5*$^{-/-}$ newborns, but only *Depdc5*$^{+/+}$ and *Depdc5*$^{+/-}$ were safely delivered (De Fusco*, Cerullo* et al., 2020). *Depdc5*$^{+/-}$ animals failed to recapitulate the major traits of the human disease, even if they showed a mild phenotype with dysmorphic pyramidal neurons and altered cortical excitability, in the absence of spontaneous seizures or increased propensity to epileptic seizures triggered by a single dose of pentylenetetrazol (Hughes et al., 2017; Marsan et al., 2016). In this context, we characterized the expression of *Depdc5* gene in a model of constitutive *Depdc5* knockout by the insertion of the Tm1a allele (**FIG. 5A**). RT-qPCR and Western Blotting were performed to evaluate the level of *Depdc5* mRNA and protein in a whole brain of E12.5 *Depdc5*$^{+/+}$, *Depdc5*$^{+/-}$ and *Depdc5*$^{-/-}$ embryos (**FIG 5B,C**). mRNA levels were halved in *Depdc5*$^{+/-}$ compared to *Depdc5*$^{+/+}$ mRNA levels and were reduced by approximately 90% in *Depdc5*$^{-/-}$ ($p<0.001$, One-Way ANOVA test). On the other hand, Depdc5 protein levels were reduced around the 50% in the heterozygous embryos, and completely absent in the homozygous (**FIG. 5C**; $p=0.002$, Student's *t*-test). Thus, despite the presence of

residual mRNA in *Depdc5*$^{-/-}$ embryos, this did not lead to protein translation, indicating the efficiency of the Tm1a allele in disrupting *Depdc5* gene expression (De Fusco*, Cerullo* et al., 2020). We next investigated mTOR activity in *Depdc5* constitutive heterozygous model by comparing the extent of S6 protein phosphorylation (pS6) in *Depdc5*$^{+/+}$ and *Depdc5*$^{+/-}$ by immunoblotting (**FIG. 5D**). Interestingly, no increase of the pS6/S6 ratio was detected when comparing *Depdc5*$^{+/-}$ and *Depdc5*$^{+/+}$. Since the presence of ectopic pS6-positive enlarged neurons is a hallmark of FCD type 2 patients, we performed an immunostaining on neuronal cultures with a phospho-specific anti-pS6 antibody (**FIG 5E**). As for the biochemical analyses, *Depdc5*$^{+/-}$ neurons were not significantly altered in both soma size and pS6/S6 ratio.

Then, we further investigate the effects of the constitutive heterozygous knockdown of *Depdc5* on synaptic transmission and intrinsic excitability. In order to characterize both excitatory and inhibitory transmissions, we recorded mEPSCs and mIPSCs on *Depdc5*$^{+/+}$ and *Depdc5*$^{+/-}$ in 14 DIV cortical neurons. Again, no changes in frequency and amplitude of mEPSCs/mIPSCs were observed in *Depdc5*$^{+/-}$ when compared to *Depdc5*$^{+/+}$ (**FIG. 6A,B**). In line with electrophysiological results, we did not observe any change in the synaptic density of both excitatory and inhibitory synapses (**FIG. 6C, upper panels**), as well as in the levels of the AMPA receptor subunit GluA1 and $GABA_A$ β2 subunit between *Depdc5*$^{+/-}$ and *Depdc5*$^{+/+}$cultures (**FIG. 6C, lower panels**). Similarly, no changes were observed in the intrinsic excitability of *Depdc5*$^{+/-}$ neurons, both in terms of number of APs elicited in 500 ms and of instantaneous frequency (**FIG. 6D**). Taken together, these data suggest the limit of *Depdc5* heterozygous animal to recapitulate the epileptic phenotype

observed in patients, and the need to loose heterozygosity in order to induce hyperactivation of mTORC1 and induce all the morphological and physiological alterations able to trigger an epileptogenic process.

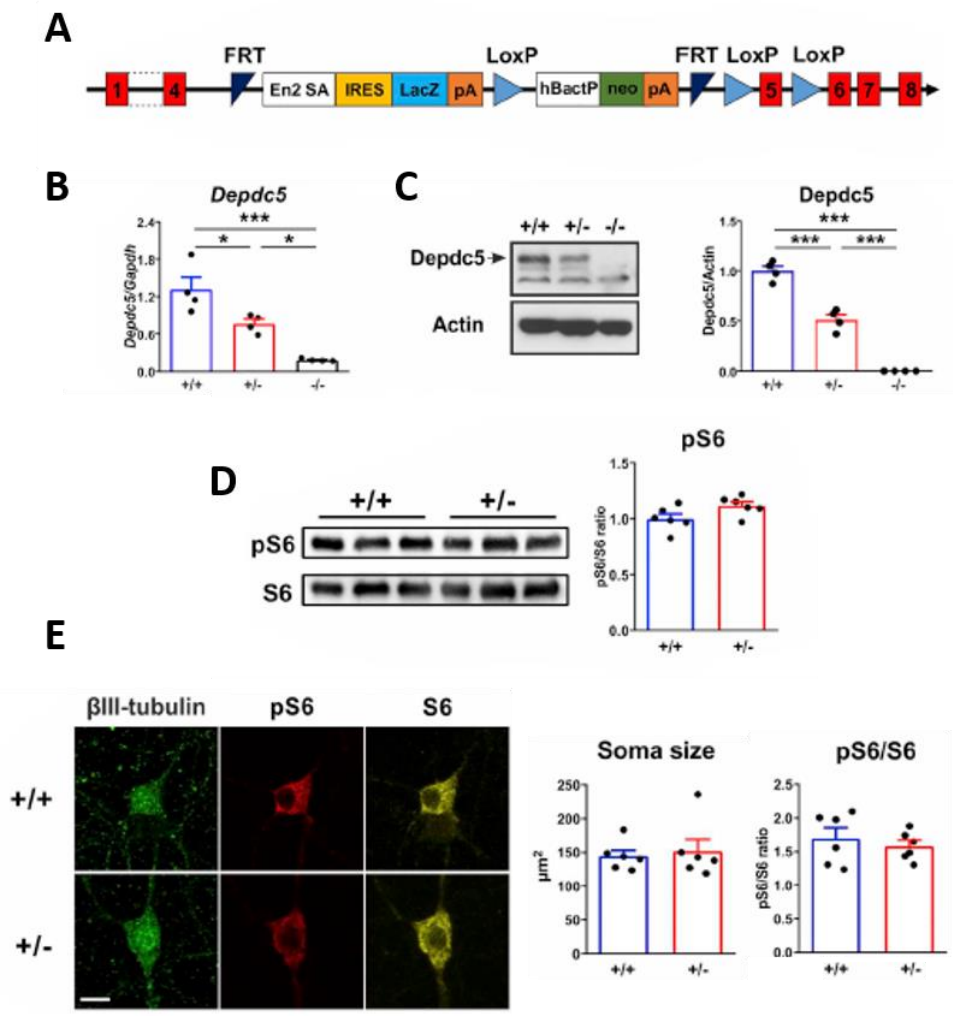

Figure 5. Characterization of the constitutive Depdc5 knockdown model. **A.** Schematic representation showing the insertion cassette of the Tm1a allele carried by *Depdc5* mouse. **B.** Bar plot showing *Depdc5* mRNA levels in *Depdc5*$^{+/+}$, *Depdc5*$^{+/-}$ and *Depdc5*$^{-/-}$ embryos (n=4). **C.** Representative Western Blot image (left) and corresponding bar plot (right) showing Depdc5 protein levels in *Depdc5*$^{+/+}$, *Depdc5*$^{+/-}$ and *Depdc5*$^{-/-}$ embryos (n=5). **D.** Representative Western Blot image (left) and quantification (right) of the pS6 levels in *Depdc5*$^{+/+}$ and *Depdc5*$^{+/-}$ in 14 DIV cortical neurons (**D**; n= 6 embryos). **E.** Representative confocal image of βIII-tubulin, pS6 and S6 staining in *Depdc5*$^{+/+}$ and *Depdc5*$^{+/-}$ (left). Bar plot showing soma size, and the fluorescent

intensity of pS6/S6 ratio in *Depdc5*$^{+/+}$ and *Depdc5*$^{+/-}$ (n = 6 plates from 3 embryos per genotype). Data are expressed as means ± SEM with individual experimental points. *p<0.05; ***p<0.001, Kruskal-Wallis ANOVA/Dunn's test (Modified from De Fusco*, Cerullo* et al., 2020).

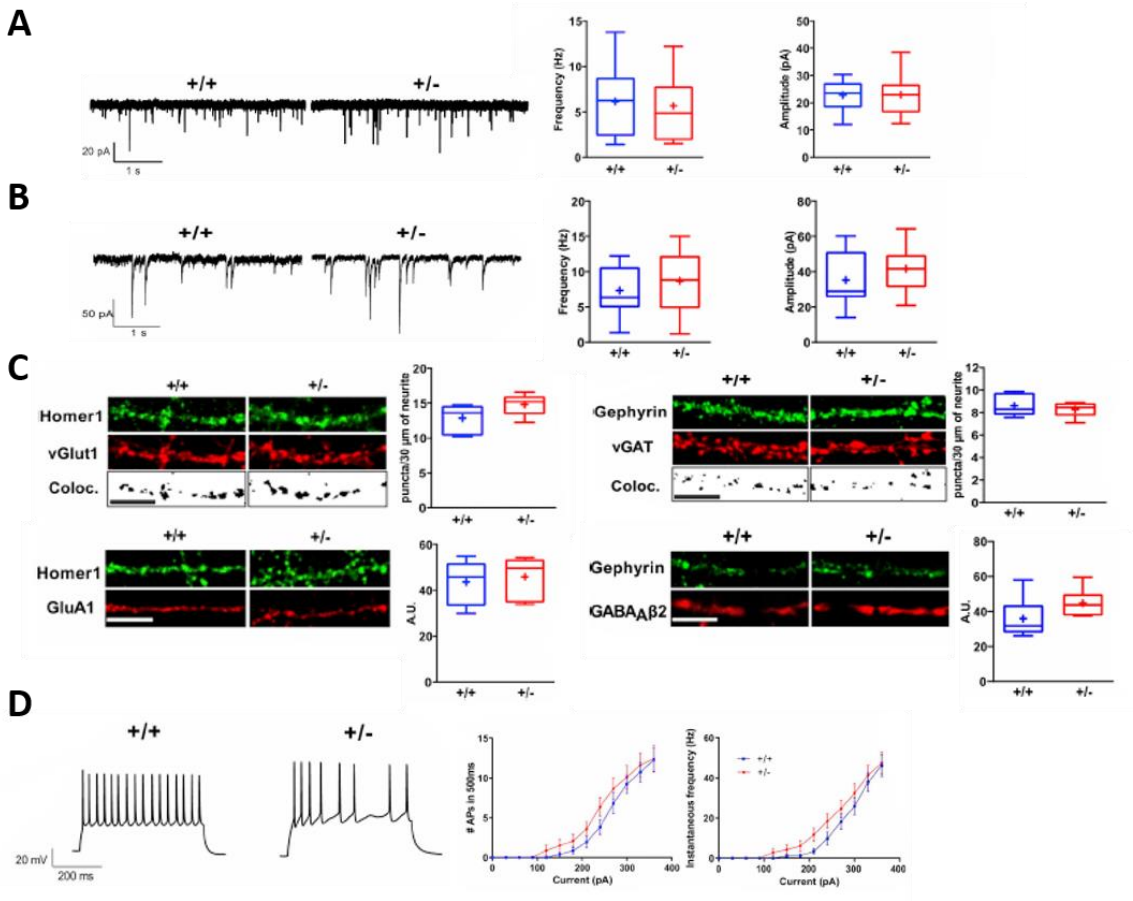

Figure 6. *Depdc5*$^{+/-}$ model fails to recapitulate the epileptogenic phenotype observed in patients. **A.** Representative traces of mEPSCs recorded in *Depdc5*$^{+/+}$ and *Depdc5*$^{+/-}$ in 14 DIV cortical neurons (left). Box plot showing the mEPSCs mean firing frequency and amplitude in *Depdc5*$^{+/+}$ (n=17) and *Depdc5*$^{+/-}$ (n=15) neurons (right). **B.** Representative traces of mIPSCs recorded in *Depdc5*$^{+/+}$ and *Depdc5*$^{+/-}$ in 14 DIV cortical neurons (left). Box plot showing the mIPSCs mean firing frequency and amplitude in *Depdc5*$^{+/+}$ (n=12) and *Depdc5*$^{+/-}$ (n=12) neurons (right). **C.** *Upper left panel*: Representative confocal images of pre/post-synaptic markers vGlut and Homer1 and box plot of the linear density of excitatory synaptic boutons quantification in *Depdc5*$^{+/+}$ and *Depdc5*$^{+/-}$ neurons. *Upper right panel:* Representative confocal images of pre/post-synaptic markers vGAT and Gephryn and box plot of the linear density of inhibitory

synaptic boutons quantification in *Depdc5*$^{+/+}$ and *Depdc5*$^{+/-}$ neurons. *Lower left panel:* Representative confocal images of the GluA1 AMPA receptor subunit at the excitatory synaptic and box plot of GluA1 AMPA receptor subunit fluorescence intensity boutons quantification in *Depdc5*$^{+/+}$ and *Depdc5*$^{+/-}$. *Lower right panel:* Representative confocal images of $GABA_A$ β2 receptor subunit at the inhibitory synaptic boutons and box plot of $GABA_A$ β2 receptor subunit fluorescence intensity boutons quantification in *Depdc5*$^{+/+}$ and *Depdc5*$^{+/-}$. **D.** Representative traces of action potential induced by injection of 270 pA for 500 ms in *Depdc5*$^{+/+}$ and *Depdc5*$^{+/-}$ neurons (left). Mean number of APs evoked at increasing level of inject current and instantaneous frequency in *Depdc5*$^{+/+}$ (n= 22) and *Depdc5*$^{+/-}$ (n= 22) neurons. All measurements were taken from n = 3 independent preparations. For histology, dendrites from at least 10 neurons per each preparation were analysed. Data are expressed as box plot and as means ± SEM. Student's *t*-test/Mann Whitney's *U*-test/ ANOVA for repeated measures. Scale bar: 10 µm (Modified from De Fusco*, Cerullo* et al., 2020).

5.2 Overcoming the limitations of the *Depdc5*$^{+/-}$ mouse model: generation and validation of the *Depdc5* conditional knockout mouse

Given the evident limitations of the *Depdc5*$^{+/-}$ mouse model to recapitulate the main features of the DEPDC5-related pathological phenotype and the need of heterozygosity loss to trigger the severe effects observed in DEPDC5 deficiency cases, we decided to focus our attention on the characterization of a conditional knockout mouse model of *Depdc5* by using the Cre/LoxP system (kindly provided by dr. Stephanie Baulac, Paris Brain Institute - Institut du Cerveau – ICM). Indeed, once obtained primary cortical neurons from *Depdc5*-floxed pups, we infected them with lentiviral vectors expressing either inactive (*Depdc5*$^{\Delta Cre}$) or active (*Depdc5*^{Cre}) Cre-recombinase at 7 DIV and performed the experiments at 14 DIV (**FIG. 7A**).

We first evaluated the level of *Depdc5* mRNA by qRT-PCR analysis in *Depdc5*$^{\Delta Cre}$ and *Depdc5*^{Cre} cortical neurons. We found that cortical neurons infected with lentivirus expressing active Cre-recombinase showed a ≈95% reduction in *Depdc5* mRNA levels compared to neurons infected with ΔCre-recombinase ($p<0.001$, Student's *t*-test; **FIG. 7B**), indicating the effective cKO of *Depdc5* through the Cre/LoxP system. In addition, Western Blot analysis also confirmed the virtual absence in Depdc5 protein levels in *Depdc5*^{Cre} compared to *Depdc5*$^{\Delta Cre}$ neurons ($p<0.001$, Student's *t*-test; **FIG. 7C**).

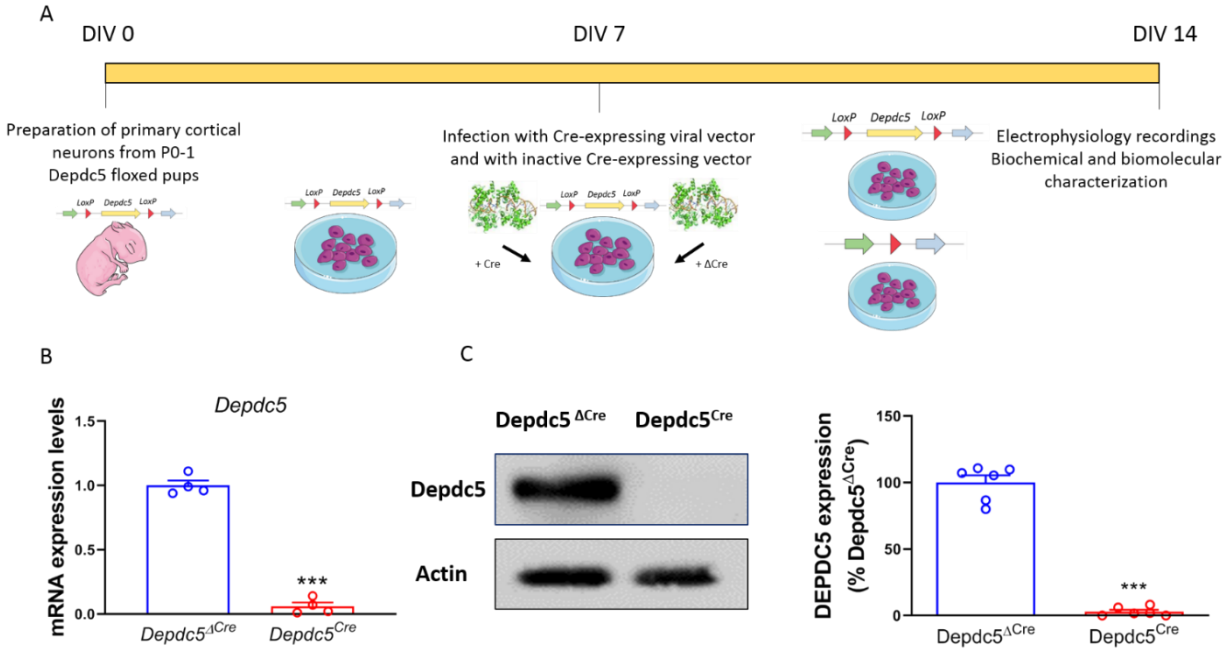

Figure 7. Experimental time course and validation of the Depdc5 cKO model. **A.** Representative scheme of the experimental design. **B.** Bar plots showing *Depdc5* mRNA levels in *Depdc5*$^{\Delta Cre}$ and *Depdc5*^{Cre} neurons, respectively (n=4 independent preparations) **C.** Representative Western Blot image (left) and corresponding bar plot of Depdc5 protein levels in *Depdc5*$^{\Delta Cre}$ and *Depdc5*^{Cre} neurons (n=6 independent preparations). Data are expressed as means ± SEM. ***p<0.001, Student's *t*-test.

5.3 Depdc5 cKO induces mTORC1 hyperactivation

Since *Depdc5* is a component of the GATOR1 complex, an upstream inhibitor of mTORC1 complex, its deletion alters the regulation of the mTORC1 pathway. To evaluate the effect of *Depdc5* cKO on this pathway, we checked for the phosphorylation level of the ribosomal protein S6 (pS6) via S6K1, that is one of the major parameter used to evaluate the level of mTORC1 activation. Indeed, *Depdc5*^{Cre} neurons displayed a significant increase of pS6 compared to *Depdc5*$^{\Delta Cre}$ neurons, while the ratio S6/actin did not change (p=0.03, Student's t-test; **FIG. 8A,B**). This indicated that the increase in the pS6 level is due to an enhanced phosphorylation by mTORC1, rather than an increase in the protein translation process (**FIG. 8B**). We also immunostained neurons with the pS6 and S6 antibodies (**FIG. 8C,D**) and, in line with the biochemical results, we observed an increase in the *Depdc5*^{Cre} pS6/S6 fluorescence intensity ratio (p=0.01, Student's *t*-test) compared to *Depdc5*$^{\Delta Cre}$ neurons. Moreover, in *Depdc5*^{Cre} neurons, we detected a significant increase soma size (p=0.03, Mann-Whitney's *U*-test), suggesting the presence of morphological alterations *in vitro* due to mTORC1 hyperactivation (**FIG. 8C,D**). Finally, we also tested whether the observed increase in S6 protein phosphorylation was actually linked to mTOR hyperactivation. To verify this hypothesis, we treated both *Depdc5*$^{\Delta Cre}$ and *Depdc5*^{Cre} neurons with rapamycin (100 nM; **FIG. 8E,F**). Interestingly, we observed a significant rescue of the *Depdc5*^{Cre} phenotype in rapamycin-treated neurons, with strong reduction of pS6 levels that became indistinguishable from those of rapamicyn-treated *Depdc5*$^{\Delta Cre}$ controls (p<0.001, 2-Way ANOVA test **FIG. 8F**). Taken

together, the data suggest that *Depdc5* cKO is required to induce hyperactivation of mTORC1 and that the loss of heterozygosity is necessary to trigger this process.

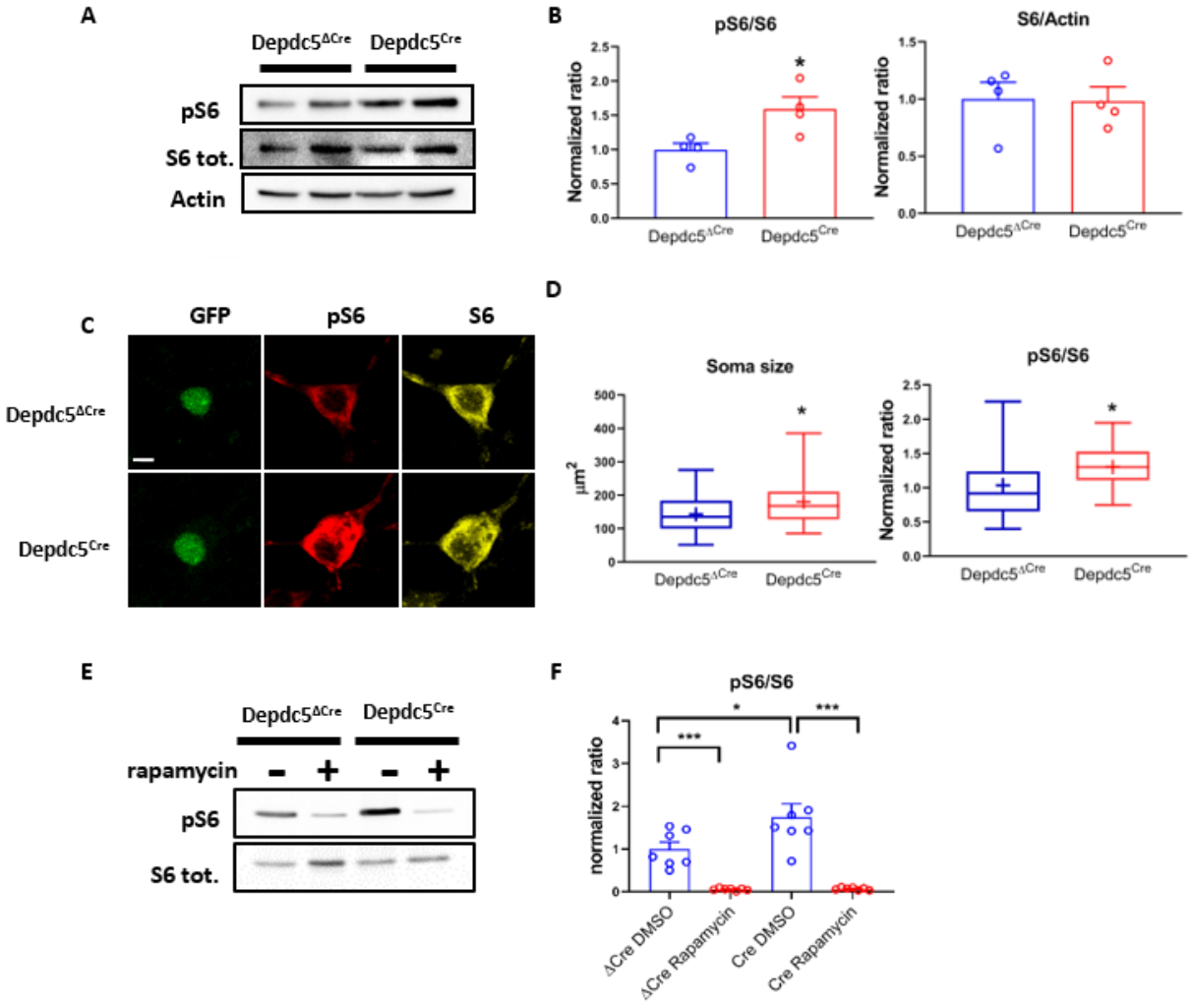

Figure 8. *Depdc5*^{Cre} neurons display hyperactivation of mTORC1 pathway and increase in soma size. **A.** Representative image of Western Blot of S6 phosphorylation in *Depdc5*$^{\Delta Cre}$ and *Depdc5*^{Cre} neurons. **B.** Bar plot representing the pS6/S6 (left) and S6/Actin ratio (n=4 independent preparations). **C.** Representative confocal image of GFP, pS6 and S6 immunofluorescence in *Depdc5*$^{\Delta Cre}$ and *Depdc5*^{Cre} neurons. **D.** Box plot showing soma size and pS6/S6 ratio in *Depdc5*$^{\Delta Cre}$ (n=33) and *Depdc5*^{Cre} (n=39) neurons. **E.** Representative image of Western Blot of S6 phosphorylation in *Depdc5*$^{\Delta Cre}$ and *Depdc5*^{Cre} neurons treated with vehicle (DMSO) and Rapamycin, respectively. **F.** Bar plot representing the pS6/S6 ratio (n=7 independent preparations). For histology, neurons from two independent preparations were analyzed. *p<0.05; **p<0.01; ***p<0.001, Student's *t*-test/Mann-Whitney's *U*-test/2-Way ANOVA test. Scale bar: 10 µm.

5.4 The *Depdc5* conditional knockout induces an increase in excitatory transmission

Imbalance between excitatory and inhibitory synaptic transmission is believed to be at the basis of most epileptic phenotypes (Bozzi et al., 2018; Stafstrom & Carmant, 2015). In the central nervous system, the mTORC1 signalling cascade is involved in the regulation of different neural processes that include neuronal differentiation, neurite outgrowth and synaptic formation during neuronal development (Bockaert & Marin, 2015; Laplante & Sabatini, 2012; Lasarge & Danzer, 2014). In particular, the balance between excitatory and inhibitory synaptic transmission have been demonstrated to be altered when mTORC1 activity is dysregulated De Fusco*, Cerullo* et al., 2020). In order to investigate this aspect, we asked whether the conditional *Depdc5* knockout could alter excitatory synaptic transmission *in vitro*. Thus, we performed electrophysiological recordings of mEPSCs and mIPSCs in in *Depdc5*$^{\Delta Cre}$ and *Depdc5*^{Cre} 14 DIV cortical neurons. Interestingly, *Depdc5*^{Cre} neurons showed a significant increase in both mEPSCs amplitude ($p<0.001$, Student's *t*-test) and mEPSCs frequency ($p=0.034$, Student's *t*-test) with respect to control *Depdc5*$^{\Delta Cre}$ neurons (**FIG. 9A,C**), in the absence of any changes in the frequency and amplitude of mIPSCs (**FIG. 9B,D**). These data further confirm the key role of *Depdc5* in regulating the excitatory/inhibitory balance at the synaptic level.

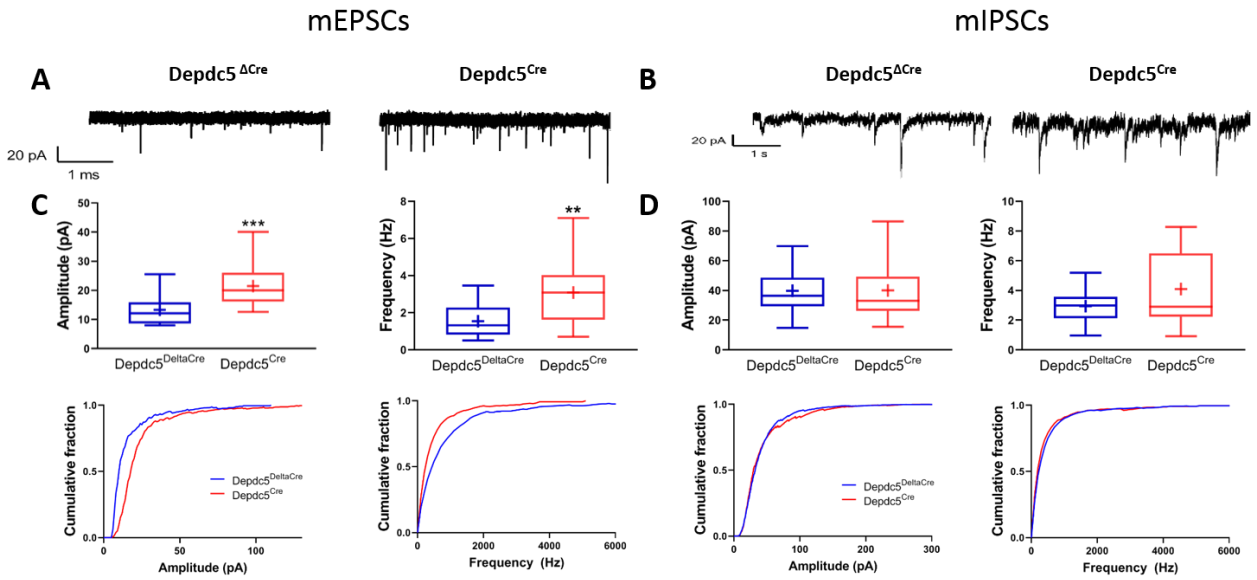

Figure 9. Conditional KO of *Depdc5* has a strong effect on spontaneous excitatory transmission, without affecting spontaneous inhibitory transmission. **A,B.** Representative traces of mEPSCs (*left*) and mIPSCs (*right*) recorded in *Depdc5*$^{\Delta Cre}$ and *Depdc5*^{Cre} primary cortical neurons. **C.** *Upper panels:* box plot showing mEPSC amplitude and frequency in *Depdc5*$^{\Delta Cre}$ (n=18) and Depdc5^{Cre} neurons (n=17). *Lower panels:* corresponding cumulative curves of amplitude and inter-event interval distribution of mEPSCs. **D.** *Upper panels:* box plot showing mIPSC amplitude and frequency in *Depdc5*$^{\Delta Cre}$ (n=19) and Depdc5^{Cre} (n=18). *Lower panels:* corresponding cumulative curves of amplitude and inter-event interval distribution of mIPSCs. All measurements were taken from n=3 independent preparations. Data are expressed as box plots. **p<0.01; ***p<0.001, Student's *t*-test.

5.5 Conditional knockout of *Depdc5* increases charge and alters the kinetics of mEPSCs

Depdc5 deficiency affects miniature excitatory postsynaptic currents, not only by increasing amplitude and frequency, but also by affecting charge and kinetics of the events (De Fusco*, Cerullo* et al., 2020). Indeed, in *Depdc5*^{Cre} neurons we observed and significant increase of the total charge transferred by the mEPSCs (p= 0.004, Student's *t*-test) when compared to the *Depdc5*$^{\Delta Cre}$ control (**FIG. 10C**). This is in line with the observed increase in amplitude, indicating an increase in the quantal size of neurotransmitter. Moreover, we observed a reduction in the 10-90 rise time (p<0.001, Mann-Whitney's *U*-test) indicating a more rapid release of the neurotransmitter quantum compared to the *Depdc5*$^{\Delta Cre}$ control (**FIG. 10C**). No differences in the mIPSCs charge, 10-90 rise time and 80% decay time were detected in *Depdc5*$^{\Delta Cre}$ and *Depdc5*^{Cre} (**FIG. 10D**).

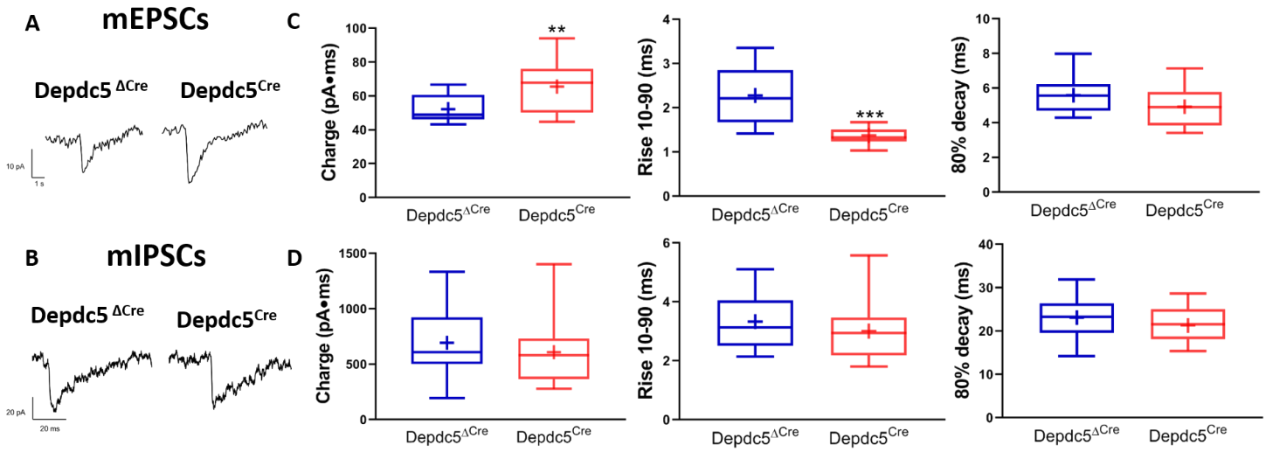

Figure 10. Depdc5 conditional KO alters mEPSC charge and 10-90 rise time. **A,B.** Representative waveforms of mEPSCs and mIPSCs recorded in *Depdc5*$^{\Delta Cre}$ and *Depdc5*^{Cre} primary cortical neurons. **C.** Box plot showing the charge (*left*), the 10-90 rise time (*middle*) and 80% decay time (*right*) parameter of mEPSCs in *Depdc5*$^{\Delta Cre}$ (n=18) and *Depdc5*^{Cre} (n=17). **D.** Box plot showing the charge (*left*), 10-90 rise time (*middle*) and 80% decay time (*right*) of mIPSCs in *Depdc5*$^{\Delta Cre}$ (n=19) and *Depdc5*^{Cre} (n=18). All measurements were taken from n=3 independent preparations. Data are expressed as box plot. **p<0.01; ***p<0.001, Student's *t*-test/Mann-Whitney's *U*-test.

5.6 Increase in number of excitatory synapses and postsynaptic receptor expression following cKO of *Depdc5*

To verify whether the changes in mEPSC frequency could be linked to variations in synaptic density, we decided to analyze the distribution of mature excitatory synapses unambiguously identified by double immunolabeling for the pre/postsynaptic markers vGlut1 and Homer1 (**FIG. 11A, left**). In agreement with the electrophysiological data, a significant increase in the density of excitatory synaptic synapses was observed in *Depdc5*^{Cre} neurons ($p<0.001$, Student's *t*-test; **Fig. 11B, left**) when compared to *Depdc5*$^{\Delta Cre}$ neurons, in parallel with the increase in mEPSC frequency. To identify mature inhibitory synapses, we performed a double immunostaining for the pre/postsynaptic markers vGAT and Gephriyn (**FIG. 11A, right**). In line with the previous electrophysiological evidence, no genotype-dependent difference in inhibitory synaptic density was observed (**FIG. 11B, right**).

We further investigated the expression of the major AMPA receptor subunit GluA1 at Homer-positive puncta, to find a possible correlation with the observed changes in mEPSC amplitude and charge (**FIG. 11C, left**). Interestingly, we found that *Depdc5*^{Cre} neurons displayed a significant increase in GluA1 fluorescence intensity compared to *Depdc5*$^{\Delta Cre}$ neurons ($p<0.001$, Student's *t*-test; **FIG. 11D, left**). We finally evaluated the expression of the $GABA_A$ β2 receptor subunit in Gephyrin-positive puncta (**FIG. 11C, right**), but no genotype-dependent difference could be found, in line with the

electrophysiological data (**FIG. 11D, right**). Overall, these data indicate a strong effect of *Depdc5* cKO on synaptic connectivity specifically affecting excitatory synapses, while inhibitory synapses appear to develop and function normally.

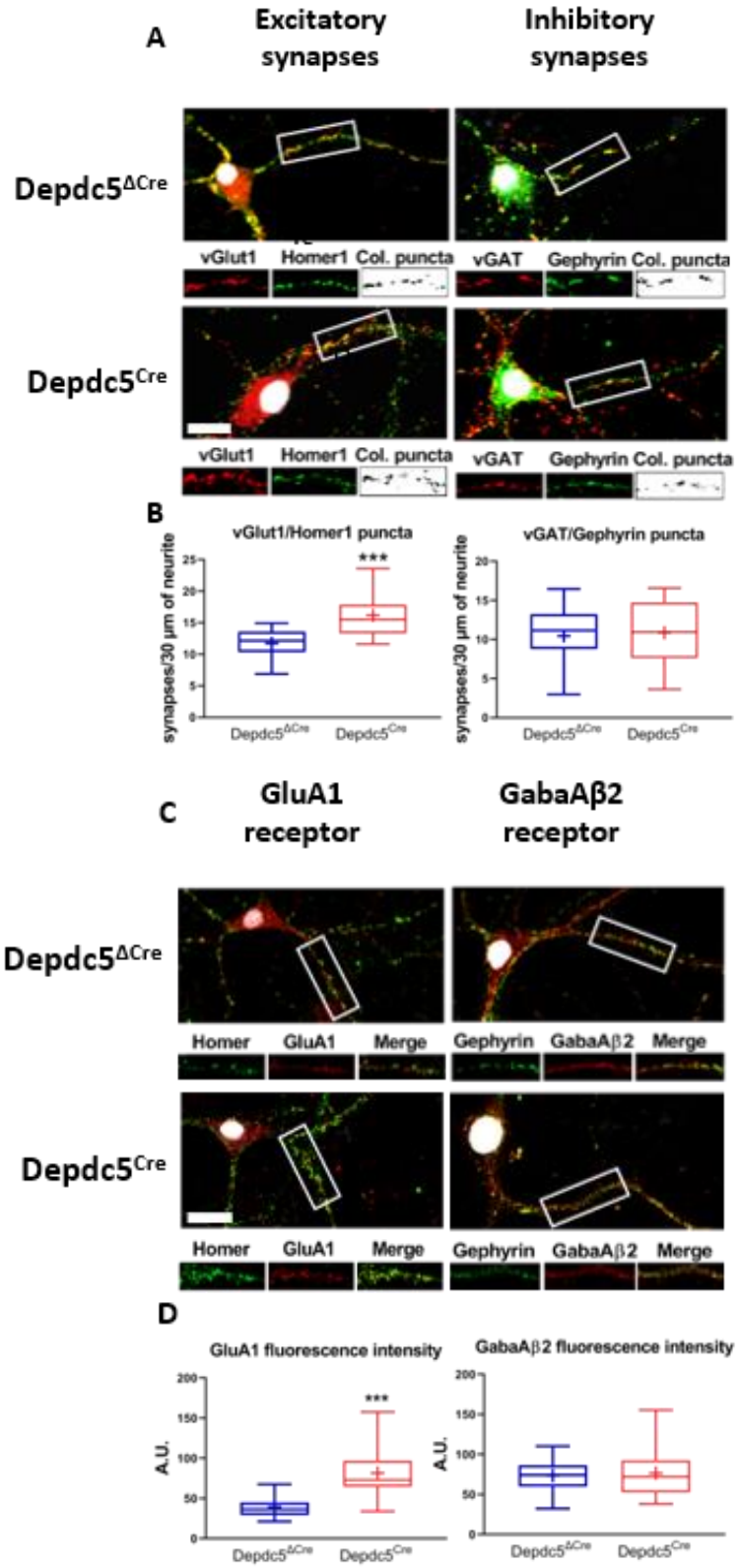
A
Excitatory synapses
Inhibitory synapses
Depdc5ΔCre
vGlut1
Homer1
Col. puncta
vGAT
Gephyrin
Col. puncta
Depdc5Cre
vGlut1
Homer1
Col. puncta
vGAT
Gephyrin
Col. puncta
B
vGlut1/Homer1 puncta
vGAT/Gephyrin puncta
synapses/30 µm of neurite
***
Depdc5ΔCre
Depdc5Cre
C
GluA1 receptor
GabaAβ2 receptor
Depdc5ΔCre
Homer
GluA1
Merge
Gephyrin
GabaAβ2
Merge
Depdc5Cre
D
GluA1 fluorescence intensity
GabaAβ2 fluorescence intensity
A.U.
***

Figure 11. *Depdc5*^{Cre} cortical neurons display an increase in the number of excitatory synaptic puncta and in the expression of the AMPA GluA1 receptor subunit. **A.** Representative confocal images of *Depdc5*$^{\Delta Cre}$ and *Depdc5*^{Cre} excitatory synaptic puncta identified by double immunostaining for vGlut1/Homer (*left*) and inhibitory synaptic puncta identified by double immunostaining for vGAT/Gephyrin (*right*). **B.** Box plots showing the quantification of the linear density of excitatory (*left*) and inhibitory (*right*) boutons in *Depdc5*$^{\Delta Cre}$ and *Depdc5*^{Cre} networks, respectively. **C.** Representative confocal images of the AMPA GluA1 receptor subunit at excitatory synapses (*left*) and of the $GABA_A$ β2 receptor subunit at inhibitory synapses (*right*) in *Depdc5*$^{\Delta Cre}$ and *Depdc5*^{Cre} neurons, respectively. **D.** Box plots showing the fluorescent intensity of the AMPA GluA1 receptor subunit (*left*) and the $GABA_A$ β2 receptor subunit (*right*) in *Depdc5*$^{\Delta Cre}$ and *Depdc5*^{Cre} neurons. For the analysis, dendrites of 20 neurons from two independent preparation were analyzed. *p<0.05, **p< 0,01, Student's *t*-test. Scale bars: 50 μm.

5.7 *Depdc5* cKO cortical neurons exhibit increased intrinsic excitability

It is known that the dysregulation to the mTORC1 pathway is linked to alteration in intrinsic excitability (De Fusco*, Cerullo* et al., 2020; Ribierre et al., 2018). In order to investigate this aspect, we performed electrophysiological recordings in current-clamp configuration to evaluate the passive and active properties of *Depdc5*$^{\Delta Cre}$ and *Depdc5*^{Cre} morphologically identified cortical pyramidal neurons. When analyzing the firing rate *versus* injected current curves in *Depdc5*$^{\Delta Cre}$ and *Depdc5*^{Cre} neurons (**FIG. 12A**), we observed an increased in the number of APs elicited during the 500 ms of current injection and in the instantaneous firing frequency in *Depdc5*^{Cre} neurons, indicating an increased intrinsic excitability (**FIG. 12C**). Interestingly, both *Depdc5*$^{\Delta Cre}$ and *Depdc5*^{Cre} did not exhibit altered passive and active properties from the phase-plane plot waveform analysis of the first elicited AP (**FIG. 13A,B, Table 1**) except for a decrease in the rheobase, i.e., in the minimum injected current needed to elicit the first AP (**FIG. 13C**). So far, these data are consistent with a condition of hyperexcitability induced by *Depdc5* cKO.

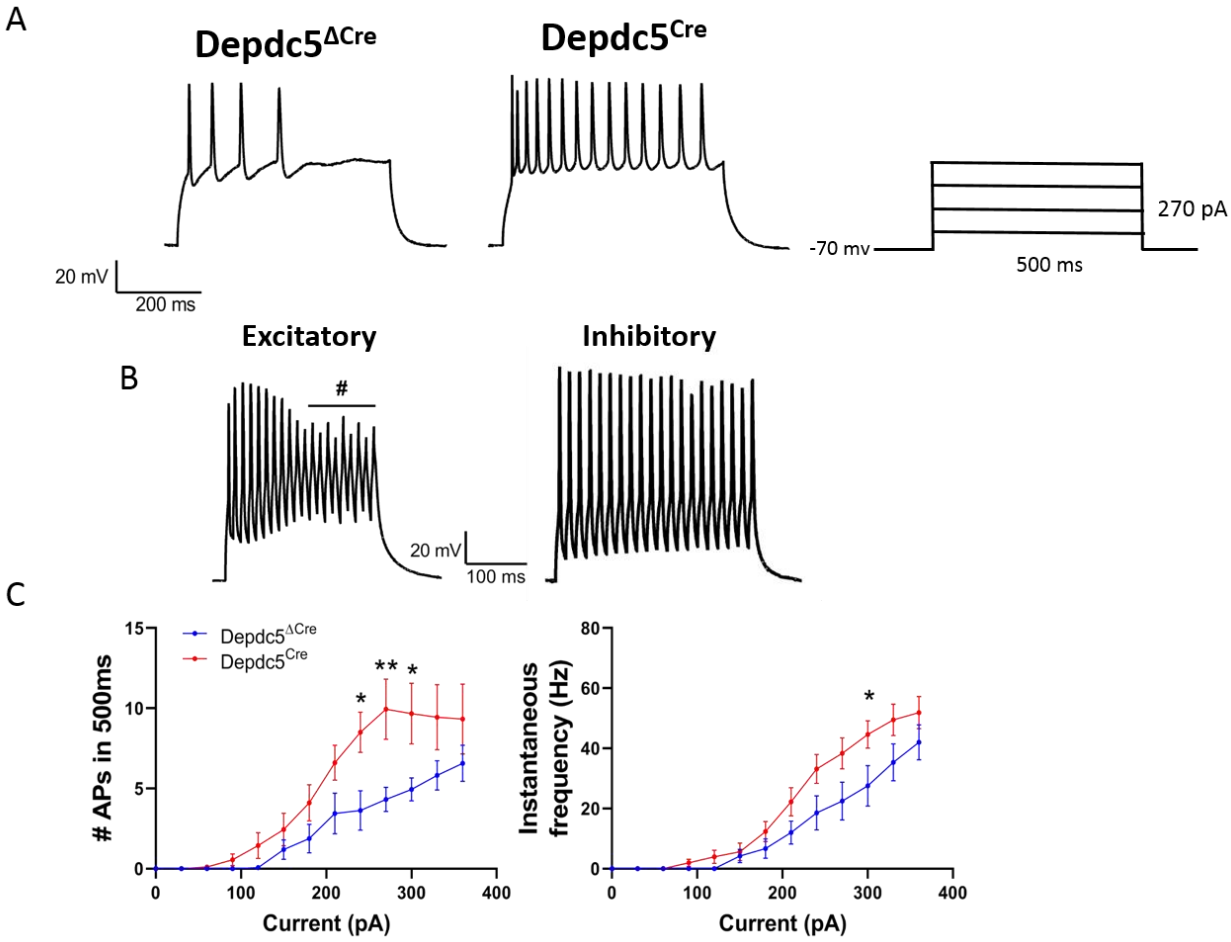

Figure 12. *Depdc5 cKO* pyramidal neurons exhibit an increased intrinsic excitability. **A.** Representative recordings of APs induced by the injection of 270 pA for 500 ms in both *Depdc5*$^{\Delta Cre}$ and *Depdc5*^{Cre} neurons and representative scheme of increasing injected current steps lasting 500 ms. **B.** Representative recordings of 20 APs evoked by 5-ms current step injection at 80 Hz used to identify excitatory neurons. Failures are labeled with #. **C.** Mean number of APs evoked by the 500 ms increasing current steps in *Depdc5*$^{\Delta Cre}$ (n=16) and *Depdc5*^{Cre} (n=18) primary pyramidal neurons *(left)* and instantaneous AP frequency *(right)*. All measurements were taken from n=3 independent preparations. Data are expressed as means ± SEM. *p<0.05, ** p< 0.01, ANOVA test for repeated measures.

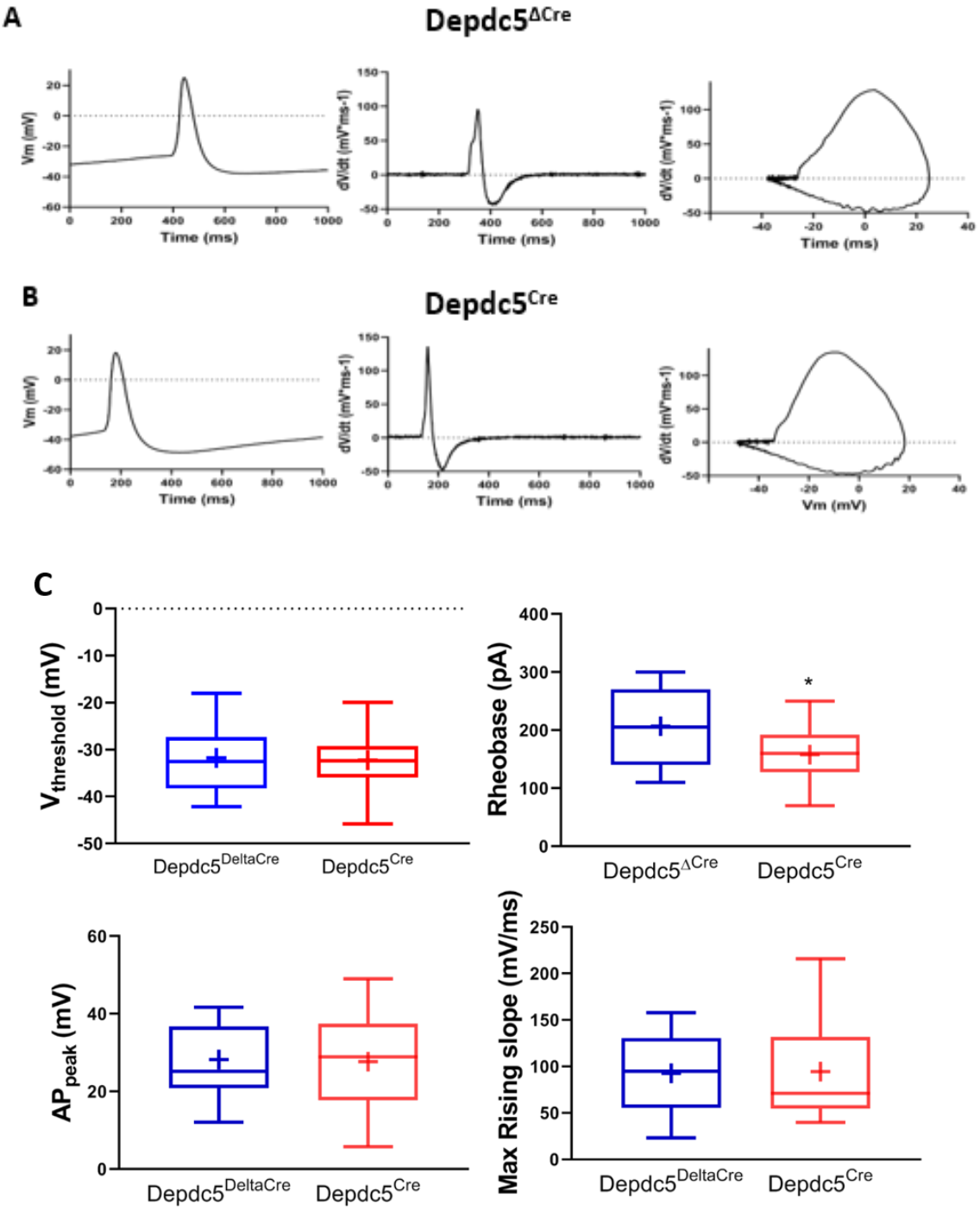
A
Depdc5ΔCre
Vm (mV)
dV/dt (mV*ms-1)
Time (ms)
B
Depdc5Cre
Vm (mV)
C
Vthreshold (mV)
Depdc5DeltaCre
Depdc5Cre
Rheobase (pA)
Depdc5ΔCre
Depdc5Cre
APpeak (mV)
Depdc5DeltaCre
Depdc5Cre
Max Rising slope (mV/ms)
Depdc5DeltaCre
Depdc5Cre

Figure 13. Depdc5 cKO does not lead to marked alterations of passive and active membrane properties. **A,B.** Representative AP (*left*), dV/dt versus time plot (*middle*) and AP phase plot (*right*) obtained from *Depdc5*$^{\Delta Cre}$ and *Depdc5*^{Cre} cortical neurons. **C.** Box plots showing $V_{threshold}$, Rheobase, AP_{peak} and Max Rising Slope parameters determined in *Depdc5*$^{\Delta Cre}$ (n=16) and *Depdc5*^{Cre} (n=18) cortical neurons. All measurements were taken from n=3 independent preparations. Data are expressed as box plot. *p<0.05, Student's *t*-test.

Table 1. Passive and active properties of Depdc5 cKO neurons.

Parameters	***Depdc5$^{\Delta Cre}$*** ***(n=16)***	***Depdc5^{Cre}*** ***(n=18)***	***p***
V_{rest} (mV)	-49.38	-51.11	0.29
C_{in} (pF)	41.98	41.84	0.50
R_{in} (MΩ)	215.6	227.8	0.70
Rheobase (pA)	209.4	157.2	0.01*
$V_{threshold}$ (mV)	-31.75	-32.22	0.84
Halfwidth (ms)	1.82	1.72	0.68
AP peak (mV)	28.21	27.62	0.87
Max rising slope (mV/ms)	92.61	94.93	0.88
Max repol. Slope (mV/ms)	-27.95	-30.32	0.53
Phase slope (ms^{-1})	8.91	8.20	0.59

Data are expressed as means ± SEM. *p<0.05; Student's t-test/Mann-Whitney's *U*-test

5.8 Depdc5 does not affect PPR and synchronous release in excitatory and inhibitory synapses

Given the strong effect of *Depdc5* cKO in triggering excitatory synaptic transmission, we asked whether it could have an effect on evoked excitatory and inhibitory postsynaptic currents (eEPSCs/eIPSCs) and short-term plasticity (STP) paradigms thereof. To investigate a possible effect on the functional properties of both type of synapses, we generated two types of primary cortical cultures. For analyzing eEPSCs and STP at the level of the excitatory transmission, we generated autaptic cell cultures (**FIG. 14A**), in which the applied stimulus and the recording evoked currents occur on the same neuron. For the inhibitory system, instead, we used a low density culture (**FIG. 14C**), in which an external stimulator was positioned on the putative presynaptic neuron, injecting current in a range of 200-500 μA. Interestingly, no significant changes in eEPSC and eIPSC amplitude were observed for both synapses in *Depdc5*$^{\Delta Cre}$ and *Depdc5*^{Cre} cortical neurons (**FIG. 14E,F; left panels**). The STP response to paired stimuli was analyzed as the ratio between two consecutive currents (I1 and I2) evoked at increasing inter-pulse intervals (from 20 ms to 1 s; paired-pulse ratio or PPR). However, no difference in the PPR ratio at all the tested interpulse intervals was observed in both excitatory and inhibitory synapses from *Depdc5*$^{\Delta Cre}$ and *Depdc5*^{Cre} (**FIG. 14E,F; right panels**). Since paired pulse plasticity is a pure presynaptic event, this result could indicate that *Dedpc5* cKO, while specifically altering synaptic connectivity of the excitatory system, has no presynaptic effects in both excitatory and inhibitory synapses.

Nevertheless, in order to deepen this hypothesis, we analyzed if the synchronous release of glutamate and GABA could be affected by the cKO of *Depdc5*. Thus, we estimated the quantal parameters of neurotransmitter release, i.e., the readily releasable pool (RRP) and the probability release (Pr) of any given synaptic vesicle in the RRP using cumulative amplitude analysis. Both excitatory and inhibitory synapses were stimulated at 40 Hz for 1s to obtain a cumulative amplitude curve (**FIG. 15A,B**). The 40 Hz train stimulation induced a significant depression of ePSCs that become evident during the stimulation period irrespective of the amplitude of the first current in the train. Thus, cumulative profile of the ePSC amplitude presents a rapid rise followed by a slower linear increase, indicating the equilibrium between depletion and constant replenishment of the RRP (**FIG. 15C,D**). The cumulative amplitude curve profile of the data points between 0.5 and 1 s were fitted by linear regression and backextrapolated to time 0 to obtain RRP value. The Pr was obtained by the ratio between the amplitude of the first event and the RRP. Again, no significant changes were observed in both of synapse types in terms of PPR and Pr (**FIG. 15E, F**), strengthening the hypothesis that *Depdc5* cKO affect excitatory synapses only at the post-synaptic level, in line with the previous data concerning the excitatory synaptic transmission. On the other hand, *Depdc5* cKO does affect inhibitory synapses, neither at the presynaptic nor at the postsynaptic level.

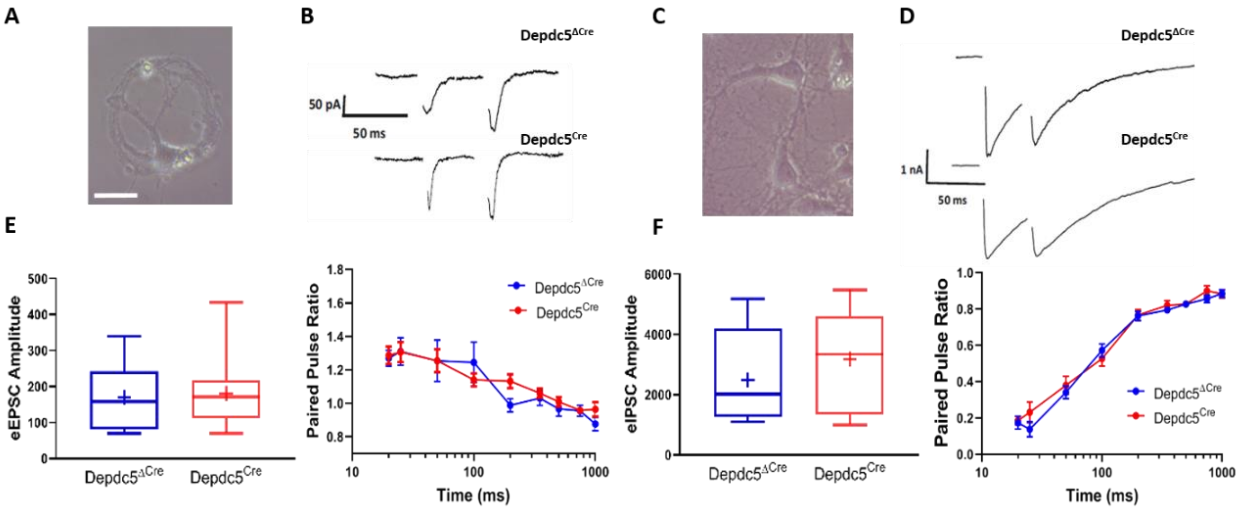

Figure 14. *Depdc5* cKO does not affect the presynaptic properties of both excitatory and inhibitory synapses. **A,B.** Representative images of autaptic neurons and representative recordings of two consecutive excitatory currents (I1 and I2) evoked at 50 ms interpulse interval in *Depdc5*$^{\Delta Cre}$ and *Depdc5*^{Cre} neurons. **C**,**D.** Representative images of pre- and postsynaptic neurons in low density cultures and representative recordings of two consecutive inhibitory currents (I1 and I2) evoked at 50 ms interpulse interval in *Depdc5*$^{\Delta Cre}$ and *Depdc5*^{Cre}. **E.** Box plot of the amplitude of eEPSCs (*left*) and paired-pulse ratio (I2/I1; *right*) of excitatory synapses at interpulse intervals from 20 ms to 1 s in *Depdc5*$^{\Delta Cre}$ (n=6) and *Depdc5*^{Cre} (n=11) neurons. **F.** Box plot of the amplitude of eIPSCs (*left*) and paired-pulse ratio (I2/I1; *right*) of inhibitory synapses at interpulse intervals from 20 ms to 1 s in *Depdc5*$^{\Delta Cre}$ (n=16) and *Depdc5*^{Cre} (n=12) neurons. All measurements were taken from n=3 independent preparations. Data are expressed as means ± SEM, ANOVA test for repeated measures.

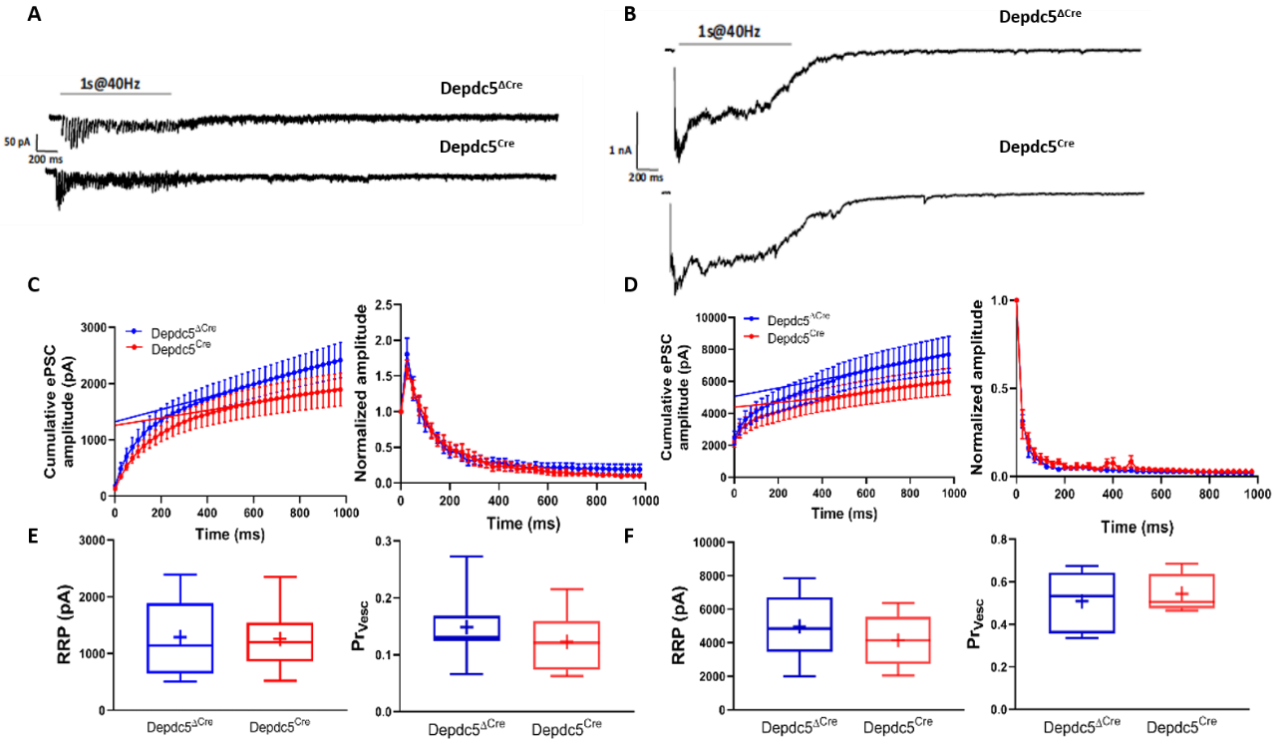

Figure 15. Depdc5 cKO does not impair synchronous release of glutamate and GABA. **A,B.** Representative traces of train stimulation at 40 Hz for 1 s in excitatory (A) and inhibitory (B) *Depdc5*$^{\Delta Cre}$ and *Depdc5*^{Cre} synapses. **C.** Cumulative eEPSC amplitude curve (*left*) and plot of normalized eEPSC amplitude *versus* time (*right*) during repetitive stimulation at 40 Hz for *Depdc5*$^{\Delta Cre}$ (n=7) and *Depdc5*^{Cre} (n=8) **D.** Cumulative eIPSC amplitude curve (left) and plot of normalized eIPSC amplitude *versus* time during repetitive stimulation at 40 Hz for *Depdc5*$^{\Delta Cre}$ (n=6) and *Depdc5*^{Cre} (n=8). **E**. Size of RRP (*left*) and calculated Pr (*right*) of excitatory synapses in *Depdc5*$^{\Delta Cre}$ (n=7) and *Depdc5*^{Cre} (n=8) neurons. **F.** Size of RRP (*left*) and calculated Pr (*right*) of inhibitory synapses in *Depdc5*$^{\Delta Cre}$ (n=6) and *Depdc5*^{Cre} (n=8) neurons. All measurements were taken from n=3 independent preparations Data are expressed as means ± SEM, Student's *t*-test/ANOVA test for repeated measures.

6. Discussion

Over the last decade, mutations in genes encoding for components of the amino acid sensing branch of the mTORC1 pathway have been involved in different forms of inherited focal epilepsies. In particular, mutations in the GATOR1 components, *NPRL2/3* and *DEPDC5* have gained more and more attention, emerging as the common cause of FEs with a phenotype ranging from sporadic early-onset epilepsies with cognitive impairment to familial focal epilepsies, and SUDEP. Among them, alterations in the *DEPDC5* gene represent the 37% of total FE cases (Baldassari et al., 2019). In view of the need of finding new therapeutic strategies for treating epilepsy, *DEPDC5* has soon become one of the most promising therapeutic targets. Nevertheless, some aspects of *Depdc5* deficiency on neuronal activity have still to be clarified (Myers & Scheffer, 2017). So far, different animal models have been generated in order to investigate the *Depdc5*-related epileptic phenotype, which is mainly characterized by an increase in the mTOR pathway activation and alteration in the cortical cytoarchitecture with abnormal and dysmorphic neurons, reminiscent of the patients' condition affected by FCD (Marsan & Baulac, 2018). Along with these altered morphological features, physiological alterations have also been described. In particular, animal models for *Depdc5*-deficiency showed excitatory/inhibitory imbalances and impaired intrinsic excitability (De Fusco*, Cerullo* et al., 2020; Klofas et al., 2020; Ribierre et al., 2018). While the heterozygous model for the *Depdc5* fails to recapitulate these aspects, it has become evident that loss of

heterozygosity is needed to trigger the *Depdc5* related-epileptic phenotype. Indeed, recent studies showed the occurrence of second-hit *DEPDC5* mutation variants in resected brain samples from individuals with FCD (Baldassari et al., 2019; Sim et al., 2019). Moreover, the temporal dynamics of *Depdc5*-loss is a fundamental part of the epileptogenic process, suggesting an important neurodevelopmental role for *Depdc5* (De Fusco*, Cerullo* et al., 2020). In this context, in order to overcome the problem of heterozygosity and have a more reliable *Depdc5*-deficiency model to deeply investigate its physiological effect on synaptic transmission and plasticity, we decided to use the Cre/LoxP system on *Depdc5*-floxed mice. In our previous work, in which we applied a post-transcriptional gene silencing strategy, we were able to induce an acute knockdown of *Depdc5* mRNA and protein, with both levels decreased around ≈80% compared to controls (De Fusco*, Cerullo* et al., 2020). Even though with this strategy *Depdc5* mRNA and protein levels were already largely reduced to a more than acceptable percentage, we decided to adopt a conditional knockout strategy by applying the Cre/LoxP system. With this strategy, the reduction of Depdc5 mRNA and protein levels were even larger, around ≈ 95%, representing a more reliable tool and model to study *Depdc5* loss effect in a more precise way both *in vitro* and in *ex vivo/in vivo* conditions. This reduction, in parallel with an increase in the mTOR activity revealed by the higher levels of pS6, is linked to an augmented excitatory neuron connectivity, characterized by increased amplitude and frequency of mEPSCs, together with an increase in the density of excitatory synapses and in the expression of postsynaptic glutamate receptors. The severe phenotype we have observed is in line with what we

previously shown in the acute *Depdc5* knockdown model by RNA interference. In this context, our data are in agreement with the excitatory/inhibitory imbalance and increased intrinsic excitability observed in other different *Depdc5*-defiency models. For example, the mosaic knockdown of *Depdc5* model showed abnormal dendritic tree growth in parallel with increased amplitude of sEPSCs and increased intrinsic excitability (Hu et al., 2018; Ribierre et al., 2018). On the other hand, Ribierre and colleagues found a reduced frequency of the spontaneous events. This is possibly due to the increased cell size with increased cell capacitance of electroporated neurons that may account for the reduced firing patterns. Nevertheless, the higher gain of firing frequency (slope F-I curve) above threshold of the electroporated *Depdc5* knockout neurons is consistent with an increase in the responsiveness to current input changes, possibly due to an alteration of ionic conductances (Ribierre et al., 2018). On the contrary, our model of *Depdc5* cKO neurons presents an increased intrinsic excitability in the absence of changes in cell capacitance; this difference is likely due to the *in vitro* conditions of our experiment.

Furthermore, our data demonstrate that only the excitatory system is affected by the *Depdc5* loss, while the inhibitory system is not significantly perturbed. This differs from previous observations in Zebrafish and in a distinct *Depdc5*^{Emx1} cKO mouse in which *Depdc5* deficiency was associated with dysregulation of the GABAergic network development (Swaminathan et al., 2018; Klofas et al., 2020). In particular, layer V pyramidal neurons of *Depdc5*^{Emx1} cKO mice show decreased mIPSC responses, suggesting a possible functional impairment in the postsynaptic response to GABAergic

inputs (Klofas et al., 2020). These discrepancies could be ascribed to the time course of *Depdc5* silencing, to species-specific differences and to the different experimental approach *(in vitro* vs. *ex vivo)* used in the experiments. All together, these data suggest that the loss of *Depdc5* heterozygosity can trigger a strong excitatory/inhibitory imbalance and an increase in intrinsic excitability that can both contribute to the epileptogenic phenotype.

Given the pivotal role in altering synaptic connectivity and intrinsic excitability, we wondered of a possible effect of *Depdc5* deficiency in synaptic plasticity. Protein synthesis is required for persistent forms of synaptic plasticity, including long-term potentiation (LTP). The mTOR pathway is known to be a key regulator of LTP-related protein synthesis by modulating the translational capacity and facilitating the synthesis of specific components of the protein synthesis machinery (Tsokas et al., 2007). Moreover, it was already reported that the mTOR pathway participates in the mechanism of LTP the CA1 in the hippocampus and that LTP in this region is a rapamycin-sensitive (Cammalleri et al., 2003).

Thus, on the basis of the reported involvement of mTOR in the mechanism of LTP and the effect of its dysregulation on synaptic transmission, we asked whether *Depdc5* loss could have an impact on short-term plasticity. We then investigated the physiological impact of *Depdc5* cKO in quantal parameters, release dynamics and STP. However, no changes were found in synaptic strength and STP in both excitatory and inhibitory synaptic transmission.

Taken together, our data suggest that the *Depdc5* loss induces mostly a change at the level of the synaptic connectivity, by increasing the number of excitatory synapses and enhancing excitatory synaptic transmission mostly at a postsynaptic level. Indeed, the increase in both amplitude and charge parameters could confirm this assumption, while the increase in the number of excitatory synaptic puncta is responsible for the increase in the mEPSCs frequency. Nevertheless, this hypothesis should be verified by further experiments evaluating possible alterations in postsynaptic dynamics.

The specific molecular mechanism underlying these functional changes triggered by *Depdc5* loss is still unclear. Interestingly, mTOR is known to have a main role in the regulation of the autophagic process. This is a very fundamental mechanism for cell physiology, since it regulates the turnover of the organelles and proteins through the endosomal system (Glick et al., 2010). In recent years, a large body of experimental evidence showed that mTOR-mediated autophagy inhibition could reduce synaptic pruning and induce internalization of glutamate receptors. In our previous model of *Depdc5* acute knockdown, we observed a significant increase in the nerve terminal endosomal area in *Depdc5*^{KD} neurons compared to the control, suggesting the existence of a defective autophagic process due to mTOR hyperactivation (De Fusco*, Cerullo* et al., 2020). Indeed, autophagy is critically involved in the molecular mechanisms underlying epileptogenesis and seizure-induced neuronal alterations. Altered autophagy reduces GABA signaling, blocks NMDAR and AMPAR degradation and induces abnormal glutamate signaling and Ca^{2+} influx (Limanaqi et al., 2020.). Furthermore, it is known that activation of mTORC1 affects synaptic activity by favoring the expression

and surface localization of AMPA receptor subunits GluA1 e GluA2, an effect that is inhibited by rapamycin (Wang et al., 2006). All this evidence represents possible scenarios through which the *Depdc5* loss, acting as a trigger for mTORC1 activity, can induce the observed phenotypes, from imbalanced excitatory/inhibitory neurotransmission to increased intrinsic excitability, all features that underlie epileptogenesis.

Technical and experimental limitation of the project. In this PhD project we show the effect of *Depdc5* cKO on primary cortical neurons by applying the Cre/LoxP technique. Even though this approach cannot be compared to the biallelic 2-hit mutational mechanism observed in patients (Ribierre et al., 2018), this subacute effect of *Depdc5* loss on primary cultures still leads to a solid neuronal phenotype. Indeed, with this model we were able to highlight the importance of the "*loss of heterozygosity*" and the neurodevelopmental role of *Depdc5.* The latter element is fundamental to trigger the changes in synaptic transmission, connectivity and structure that are associated with mTOR hyperactivation and related epileptogenesis, as shown in this dissertation and in our previous model of *Depdc5* acute knock-down (De Fusco*, Cerullo* et al., 2020).

Despite the severe phenotype observed in the *Depdc5* cKO model, characterized through electrophysiological, biomolecular and biochemical experiments, the important missing piece is the understanding of specific mechanism of action of *Depdc5* loss. We still need (i) to clarify whether the observed phenotypes are due to alterations at the transcriptional level, in the interactions with different signal transduction systems or to

complex dysregulations in protein expression and (ii) to define how *Depdc5* loss-of-function can influence these processes.

The mTOR signaling pathway is composed of different upstream and downstream regulators that interact one with each other. Thus, understanding the precise mechanisms through which the *Depdc5* loss impact the activity of the mTOR signaling pathway is still a challenging open question.

7. Conclusions and future perspectives

In this dissertation we showed how *Depdc5* cKO induces a strong alteration of excitatory synaptic transmission and intrinsic excitability, two effects that can synergistically trigger the epileptogenic process through the establishment of an excitation/inhibition imbalance. Moreover, our data suggest that the effect of *Depdc5* loss mainly consists of an increase of excitatory synaptic connections, with increased postsynaptic glutamate receptors, without apparently affecting short-term synaptic plasticity that mostly relies on presynaptic mechanisms. Further experiments are still needed to verify this hypothesis. Indeed, other STP paradigms and glutamate puff recordings will be performed to deepen the role of *Depdc5* loss on synaptic plasticity and to assess the contribution of *Depdc5* to glutamate transmission at the postsynaptic level. Together with these electrophysiological data, further biochemical assay, such as biotinylation of AMPA receptors will be performed, in order to better characterize the mechanistic role of *Depdc5* in excitatory synaptic transmission, an important missing piece in the understanding of the effects of *Depdc5* loss on neuronal activity. Moreover, given the pivotal role of mTOR pathway in regulating LTP, it would also be interesting to assess the impact of *Depdc5* loss on long-term plasticity phenomena, that involve protein synthesis and variation in synaptic connectivity.

Overall, our data confirm the idea that the loss of heterozygosity, and thus a significant increase in mTOR activity, is necessary to trigger the *Dedpc5*-related epileptogenic phenotype that likely consists of a developmental effect at the level of synaptic connections that is associated with a strong E/I imbalance and intrinsic hyperexcitability. In this context, our data help to understand the physiological role of *Depdc5* and the pathomechanisms by which *Depdc5* loss triggers epileptogenesis, representing a starting point for further investigations and indicating this gene as potential target for new therapeutic strategies for GATOR1-related neurological disorders.

8. Acknowledgements

At the end of my PhD I would like to thank all the people that supported me to complete this important journey and I would like to express them all my gratitude.

First, I would like to thank my supervisor, Professor Fabio Benfenati for his invaluable mentoring and supervision, and the essential help for the developing of the project.

I thank Professor Pietro Baldelli for the precious discussions and suggestions for electrophysiological experiments.

A special thank to Dr. Stephanie Baulac and Dr. Gabriele Lignani for their useful thesis revision and comments.

I thank Dr. Antonio De Fusco for the biochemical and biomolecular experiments, but especially for the constructive support and discussion on the project.

I thank all the NSYN team and my PhD fellows, you are too many to be named, but just know that sharing this experience with you made it even more special. Thank you for all the unforgettable moments together.

I would like to thank my friends Alessia and Irene, who are always with me no matter how distant we are.

Thanks to all the beautiful people I have met in all these years in Genova, precious friends that I will always carry in my heart.

Last but not the least, I would like to express my immense gratitude to my parents, for their never-ending support and love. A special thank to Sam, for encouraging me throughout these last years of PhD, for his support and love.

9. References

Baldassari, S., Licchetta, L., Tinuper, P., Bisulli, F., & Pippucci, T. (2016). GATOR1 complex: The common genetic actor in focal epilepsies. *Journal of Medical Genetics*, *53*(8), 503–510. https://doi.org/10.1136/jmedgenet-2016-103883

Baldassari, S., Picard, F., Verbeek, N. E., van Kempen, M., Brilstra, E. H., Lesca, G., … Baulac, S. (2019). The landscape of epilepsy-related GATOR1 variants. *Genetics in Medicine*, *21*(2), 398–408. https://doi.org/10.1038/s41436-018-0060-2

Bar-Peled, L., Chantranupong, L., Cherniack, A. D., Chen, W. W., Ottina, K. A., Grabiner, B. C., … Sabatini, D. M. (2013). A tumor suppressor complex with GAP activity for the Rag GTPases that signal amino acid sufficiency to mTORC1. *Science*, *340*(6136), 1100–1106. https://doi.org/10.1126/science.1232044

Bateup, H. S., Johnson, C. a, Denefrio, C. L., Saulnier, J. L., & Sabatini, B. L. (2013). hyperexcitability in mouse models of Tuberous Sclerosis. *Neuron*, *78*(3), 510–522. https://doi.org/10.1016/j.neuron.2013.03.017.Excitatory/inhibitory

Baulac, S. (2014). Genetics advances in autosomal dominant focal epilepsies: Focus on DEPDC5. *Progress in Brain Research*, *213*(C), 123–139. https://doi.org/10.1016/B978-0-444-63326-2.00007-7

Beaudoin, G. M. J., Lee, S. H., Singh, D., Yuan, Y., Ng, Y. G., Reichardt, L. F., & Arikkath, J. (2012). Culturing pyramidal neurons from the early postnatal mouse hippocampus and cortex. *Nature Protocols*, *7*(9), 1741–1754. https://doi.org/10.1038/nprot.2012.099

Berg, A. T., Berkovic, S. F., Brodie, M. J., Buchhalter, J., Cross, J. H., Van Emde Boas, W., … Scheffer, I. E. (2010). Revised terminology and concepts for organization of seizures and epilepsies: Report of the ILAE Commission on Classification and Terminology, 2005-2009. *Epilepsia*, *51*(4), 676–685. https://doi.org/10.1111/j.1528-1167.2010.02522.x

Bockaert, J., & Marin, P. (2015). mTOR in brain physiology and pathologies. *Physiological Reviews*, *95*(4), 1157–1187. https://doi.org/10.1152/physrev.00038.2014

Boillot, M., & Baulac, S. (2016). Genetic models of focal epilepsies. *Journal of Neuroscience Methods*, *260*, 132–143. https://doi.org/10.1016/j.jneumeth.2015.06.003

Bozzi, Y., Provenzano, G., & Casarosa, S. (2018). Neurobiological bases of autism–epilepsy comorbidity: a focus on excitation/inhibition imbalance. *European Journal of Neuroscience*, *47*(6), 534–548. https://doi.org/10.1111/ejn.13595

Cammalleri, M., Lü tjens, R., Berton, F., King, A. R., Simpson, C., Francesconi, W., & Paolo Sanna, P. (2003). *Time-restricted role for dendritic activation of the mTOR-p70 S6K pathway in the induction of late-phase long-term potentiation in the CA1*. Retrieved from www.pnas.orgcgidoi10.1073pnas.2336098100

Catterall, W. A. (2013). Sodium Channel Mutations and Epilepsy. In *Jasper's Basic Mechanisms of the Epilepsies* (pp. 675–687). Oxford University Press. https://doi.org/10.1093/med/9780199746545.003.0052

Chiappalone, M., Casagrande, S., Tedesco, M., Valtorta, F., Baldelli, P., Martinoia, S., & Benfenati, F. (2009). Opposite changes in glutamatergic and GABAergic transmission underlie the diffuse hyperexcitability of synapsin i-deficient cortical networks. *Cerebral Cortex*, *19*(6), 1422–1439. https://doi.org/10.1093/cercor/bhn182

Citraro, R., Leo, A., Constanti, A., Russo, E., & De Sarro, G. (2016). MTOR pathway inhibition as a new therapeutic strategy in epilepsy and epileptogenesis. *Pharmacological Research*, *107*, 333–343. https://doi.org/10.1016/j.phrs.2016.03.039

Colasante, G., Qiu, Y., Massimino, L., Berardino, C. Di, Cornford, J. H., Snowball, A., … Lignani, G. (n.d.). In vivo CRISPRa decreases seizures and rescues cognitive deficits in a rodent model of epilepsy. https://doi.org/10.1093/brain/awaa045

de Calbiac, H., Dabacan, A., Marsan, E., Tostivint, H., Devienne, G., Ishida, S., … Ciura, S. (2018). Depdc5 knockdown causes mTOR-dependent motor hyperactivity in zebrafish. *Annals of Clinical and Translational Neurology*, *5*(5), 510–523. https://doi.org/10.1002/acn3.542

De Fusco*, A., Cerullo*, M. S., Marte, A., Michetti, C., Romei, A., Castroflorio, E., … Benfenati, F. (2020). Acute knockdown of Depdc5 leads to synaptic defects in mTOR-related epileptogenesis. *Neurobiology of Disease*, *139*, 104822. https://doi.org/10.1016/j.nbd.2020.104822

Devinsky, O., Vezzani, A., O'Brien, T. J., Jette, N., Scheffer, I. E., De Curtis, M., & Perucca, P. (2018). Epilepsy. *Nature Reviews Disease Primers*, *4*(May). https://doi.org/10.1038/nrdp.2018.24

Dezsi, G., Ozturk, E., Stanic, D., Powell, K. L., Blumenfeld, H., O'Brien, T. J., & Jones, N. C. (2013). Ethosuximide reduces epileptogenesis and behavioral comorbidity in the GAERS model of genetic generalized epilepsy. *Epilepsia*, *54*(4), 635–643. https://doi.org/10.1111/epi.12118

Dibbens, L. M., De Vries, B., Donatello, S., Heron, S. E., Hodgson, B. L., Chintawar, S., … Scheffer, I. E. (2013). Mutations in DEPDC5 cause familial focal epilepsy with variable foci. *Nature Genetics*, *45*(5), 546–551. https://doi.org/10.1038/ng.2599

Falco-Walter, J. J., Scheffer, I. E., & Fisher, R. S. (2018). The new definition and classification of seizures and epilepsy. *Epilepsy Research*, *139*(November 2017), 73–79. https://doi.org/10.1016/j.eplepsyres.2017.11.015

Fisher, R. S., Acevedo, C., Arzimanoglou, A., Bogacz, A., Cross, J. H., Elger, C. E., … Wiebe, S. (2014). ILAE Official Report: A practical clinical definition of epilepsy. *Epilepsia*, *55*(4), 475–482. https://doi.org/10.1111/epi.12550

Fisher, R. S., Cross, J. H., French, J. A., Higurashi, N., Hirsch, E., Jansen, F. E., … Zuberi, S. M. (2017). Operational classification of seizure types by the International League Against Epilepsy: Position Paper of the ILAE Commission for Classification and Terminology. *Epilepsia*, *58*(4), 522–530. https://doi.org/10.1111/epi.13670

Fishwick, K. J., Li, R. A., Halley, P., Deng, P., & Storey, K. G. (2010). Initiation of neuronal differentiation requires PI3-kinase/TOR signalling in the vertebrate neural tube. *Developmental Biology*, *338*(2), 215–225. https://doi.org/10.1016/j.ydbio.2009.12.001

French, J. A., Lawson, J. A., Yapici, Z., Ikeda, H., Polster, T., Nabbout, R., … Franz, D. N. (2016). Adjunctive everolimus therapy for treatment-resistant focal-onset seizures associated with tuberous sclerosis (EXIST-3): a phase 3, randomised, double-blind, placebo-controlled study. *The Lancet*, *388*(10056), 2153–2163. https://doi.org/10.1016/S0140-6736(16)31419-2

Gastaut, H. (1970). Clinical and Electroencephalographical Classification of Epileptic Seizures. *Epilepsia*, *11*(1), 102–112. https://doi.org/10.1111/j.1528-1157.1970.tb03871.x

Glick, D., Barth, S., & Macleod, K. F. (2010, May 1). Autophagy: Cellular and molecular mechanisms. *Journal of Pathology*. John Wiley & Sons, Ltd. https://doi.org/10.1002/path.2697

González, A., & Hall, M. N. (2017). Nutrient sensing and TOR signaling in yeast and mammals . *The EMBO Journal*, *36*(4), 397–408. https://doi.org/10.15252/embj.201696010

Gregorian, C., Nakashima, J., Belle, J. Le, Ohab, J., Kim, R., Liu, A., … Wu, H. (2009). Pten deletion in adult neural stem/progenitor cells enhances constitutive neurogenesis. *Journal of Neuroscience*, *29*(6), 1874–1886. https://doi.org/10.1523/JNEUROSCI.3095-08.2009

Griffith, J. L., & Wong, M. (2018). The mTOR pathway in treatment of epilepsy: A clinical update. *Future Neurology*, *13*(2), 49–58. https://doi.org/10.2217/fnl-2018-0001

Henshall, D. C., & Kobow, K. (2015). Epigenetics and epilepsy. *Cold Spring Harbor Perspectives in Medicine*, *5*(12). https://doi.org/10.1101/cshperspect.a022731

Hu, S., Knowlton, R. C., Watson, B. O., Glanowska, K. M., Murphy, G. G., Parent, J. M., & Wang, Y. (2018). Somatic Depdc5 deletion recapitulates electroclinical features of human focal cortical dysplasia type IIA. *Annals of Neurology*, *84*(1), 140–146. https://doi.org/10.1002/ana.25272

Hughes, J., Dawson, R., Tea, M., McAninch, D., Piltz, S., Jackson, D., … Thomas, P. (2017). Knockout of the epilepsy gene Depdc5 in mice causes severe embryonic dysmorphology with hyperactivity of mTORC1 signalling. *Scientific Reports*, *7*(1), 1–15. https://doi.org/10.1038/s41598-017-12574-2

Ishida, S., Picard, F., Rudolf, G., Noé, E., Achaz, G., Thomas, P., … Baulac, S. (2013). Mutations of DEPDC5 cause autosomal dominant focal epilepsies. *Nature Genetics*, *45*(5), 552–555. https://doi.org/10.1038/ng.2601

Jaudon, F., Chiacchiaretta, M., Albini, M., Ferroni, S., Benfenati, F., & Cesca, F. (2020). Kidins220/ARMS controls astrocyte calcium signaling and neuron–astrocyte communication. *Cell Death and Differentiation*, *27*(5), 1505–1519. https://doi.org/10.1038/s41418-019-0431-5

Jaworski, J., Spangler, S., Seeburg, D. P., Hoogenraad, C. C., & Sheng, M. (2005). Control of dendritic arborization by the phosphoinositide-3'-kinase- Akt-mammalian target of rapamycin pathway. *Journal of Neuroscience*, *25*(49), 11300–11312. https://doi.org/10.1523/JNEUROSCI.2270-05.2005

Kaeser, P. S., Deng, L., Wang, Y., Dulubova, I., Liu, X., Rizo, J., & Südhof, T. C. (2011). RIM

proteins tether Ca2+ channels to presynaptic active zones via a direct PDZ-domain interaction. *Cell*, *144*(2), 282–295. https://doi.org/10.1016/j.cell.2010.12.029

Klofas, L. K., Short, B. P., Zhou, C., & Carson, R. P. (2020). Prevention of premature death and seizures in a Depdc5 mouse epilepsy model through inhibition of mTORC1. *Human Molecular Genetics*, *29*(8), 1365–1377. https://doi.org/10.1093/hmg/ddaa068

Kullmann, D. M., Schorge, S., Walker, M. C., & Wykes, R. C. (2014). Gene therapy in epilepsy - Is it time for clinical trials? *Nature Reviews Neurology*. Nature Publishing Group. https://doi.org/10.1038/nrneurol.2014.43

Kwan, P., & Brodie, M. J. (2006). Refractory epilepsy: Mechanisms and solutions. *Expert Review of Neurotherapeutics*, *6*(3), 397–406. https://doi.org/10.1586/14737175.6.3.397

Laplante, M., & Sabatini, D. M. (2012, April 13). MTOR signaling in growth control and disease. *Cell*. Cell. https://doi.org/10.1016/j.cell.2012.03.017

Lasarge, C. L., & Danzer, S. C. (2014). Mechanisms regulating neuronal excitability and seizure development following mTOR pathway hyperactivation. *Frontiers in Molecular Neuroscience*, *7*(MAR), 1–15. https://doi.org/10.3389/fnmol.2014.00018

Limanaqi, F., Biagioni, F., Letizia Busceti, C., Fabrizi, C., Frati, A., & Fornai, F. (n.d.). Molecular Sciences mTOR-Related Cell-Clearing Systems in Epileptic Seizures, an Update. https://doi.org/10.3390/ijms21051642

Malagelada, C., Angel López-Toledano, M., Willett, R. T., Jin, Z. H., Shelanski, M. L., & Greene, L. A. (2011). Development/Plasticity/Repair RTP801/REDD1 Regulates the Timing of Cortical Neurogenesis and Neuron Migration. https://doi.org/10.1523/JNEUROSCI.4011-10.2011

Marsan, E., & Baulac, S. (2018, February 1). Review: Mechanistic target of rapamycin (mTOR) pathway, focal cortical dysplasia and epilepsy. *Neuropathology and Applied Neurobiology*. Blackwell Publishing Ltd. https://doi.org/10.1111/nan.12463

Marsan, Elise, Ishida, S., Schramm, A., Weckhuysen, S., Muraca, G., Lecas, S., … Baulac, S. (2016). Depdc5 knockout rat: A novel model of mTORopathy. *Neurobiology of Disease*, *89*, 180–189. https://doi.org/10.1016/j.nbd.2016.02.010

Mula, M. (2016). Investigational new drugs for focal epilepsy. *Expert Opinion on Investigational Drugs*, *25*(1), 1–5. https://doi.org/10.1517/13543784.2016.1110144

Mula, M. (2018). Emerging drugs for focal epilepsy. *Expert Opinion on Emerging Drugs*, *23*(3), 243–249. https://doi.org/10.1080/14728214.2018.1527903

Myers, K. A., & Scheffer, I. E. (2017). DEPDC5 as a potential therapeutic target for epilepsy. *Expert Opinion on Therapeutic Targets*, *21*(6), 591–600. https://doi.org/10.1080/14728222.2017.1316715

Ottman, R., Winawer, M. R., Kalachikov, S., Barker-Cummings, C., Gilliam, T. C., Pedley, T. A., & Hauser, W. A. (2004). LGI1 mutations in autosomal dominant partial epilepsy with auditory features. *Neurology*, *62*(7), 1120–1126. https://doi.org/10.1212/01.WNL.0000120098.39231.6E

Pack, A. M. (2019). Epilepsy Overview and Revised Classification of Seizures and Epilepsies.

CONTINUUM Lifelong Learning in Neurology, *25*(2), 306–321. https://doi.org/10.1212/CON.0000000000000707

Prestigio, C., Ferrante, D., Valente, P., Casagrande, S., Albanesi, E., Yanagawa, Y., … Baldelli, P. (2019). Spike-Related Electrophysiological Identification of Cultured Hippocampal Excitatory and Inhibitory Neurons. *Molecular Neurobiology*, *56*(9), 6276–6292. https://doi.org/10.1007/s12035-019-1506-5

Raab-Graham, K. F., Haddick, P. C. G., Jan, Y. N., & Jan, L. Y. (2006). Activity- and mTOR-dependent suppression of Kv1.1 channel mRNA translation in dendrites. *Science*, *314*(5796), 144–148. https://doi.org/10.1126/science.1131693

Ribierre, T., Deleuze, C., Bacq, A., Baldassari, S., Marsan, E., Chipaux, M., … Baulac, S. (2018). Second-hit mosaic mutation in mTORC1 repressor DEPDC5 causes focal cortical dysplasia-associated epilepsy. *Journal of Clinical Investigation*, *128*(6), 2452–2458. https://doi.org/10.1172/JCI99384

Ricos, M. G., Hodgson, B. L., Pippucci, T., Saidin, A., Ong, Y. S., Heron, S. E., … Dibbens, L. M. (2016). Mutations in the mammalian target of rapamycin pathway regulators NPRL2 and NPRL3 cause focal epilepsy. *Annals of Neurology*, *79*(1), 120–131. https://doi.org/10.1002/ana.24547

Ryther, R. C. C., & Wong, M. (2012). Mammalian target of rapamycin (mtor) inhibition: Potential for antiseizure, antiepileptogenic, and epileptostatic therapy. *Current Neurology and Neuroscience Reports*, *12*(4), 410–418. https://doi.org/10.1007/s11910-012-0276-5

Sadowski, K., Kotulska-Jóźwiak, K., & Jóźwiak, S. (2015). Role of mTOR inhibitors in epilepsy treatment. *Pharmacological Reports*, *67*(3), 636–646. https://doi.org/10.1016/j.pharep.2014.12.017

Sancak, Y., Peterson, T. R., Shaul, Y. D., Lindquist, R. A., Thoreen, C. C., Bar-Peled, L., & Sabatini, D. M. (2008). The rag GTPases bind raptor and mediate amino acid signaling to mTORC1. *Science*, *320*(5882), 1496–1501. https://doi.org/10.1126/science.1157535

Scheffer, I. E., Berkovic, S., Capovilla, G., Connolly, M. B., French, J., Guilhoto, L., … Zuberi, S. M. (2017). ILAE classification of the epilepsies: Position paper of the ILAE Commission for Classification and Terminology. *Epilepsia*, *58*(4), 512–521. https://doi.org/10.1111/epi.13709

Schneggenburger, R., Meyer, A. C., & Neher, E. (1999). Released fraction and total size of a pool of immediately available transmitter quanta at a calyx synapse. *Neuron*, *23*(2), 399–409. https://doi.org/10.1016/S0896-6273(00)80789-8

Shen, K., Huang, R. K., Brignole, E. J., Condon, K. J., Valenstein, L., Chantranupong, L., … Sabatini, D. M. (2018). HHS Public Access, *556*(7699), 64–69. https://doi.org/10.1038/nature26158.Architecture

Sim, J. C., Scerri, T., Fanjul-Fernández, M., Riseley, J. R., Gillies, G., Pope, K., … Leventer, R. J. (2016). Familial cortical dysplasia caused by mutation in the mammalian target of rapamycin regulator NPRL3. *Annals of Neurology*, *79*(1), 132–137. https://doi.org/10.1002/ana.24502

Sim, N. S., Ko, A., Kim, W. K., Kim, S. H., Kim, J. S., Shim, K. W., … Lee, J. H. (2019). Precise detection of low-level somatic mutation in resected epilepsy brain tissue. *Acta Neuropathologica*, *138*(6), 901–912. https://doi.org/10.1007/s00401-019-02052-6

Skarnes, W. C., Rosen, B., West, A. P., Koutsourakis, M., Bushell, W., Iyer, V., … Bradley, A. (2011). A conditional knockout resource for the genome-wide study of mouse gene function. *Nature*, *474*(7351), 337–344. https://doi.org/10.1038/nature10163

Stafstrom, C. E., & Carmant, L. (2015). Seizures and epilepsy: An overview for neuroscientists. *Cold Spring Harbor Perspectives in Biology*, *7*(5), 1–19. https://doi.org/10.1101/cshperspect.a022426

Steinlein, O. K., Mulley, J. C., Propping, P., Wallace, R. H., Phillips, H. A., Sutherland, G. R., … Berkovic, S. F. (1995). A missense mutation in the neuronal nicotinic acetylcholine receptor α4 subunit is associated with autosomal dominant nocturnal frontal lobe epilepsy. *Nature Genetics*, *11*(2), 201–203. https://doi.org/10.1038/ng1095-201

Swaminathan, A., Hassan-Abdi, R., Renault, S., Siekierska, A., Riché, R., Liao, M., … Samarut, É. (2018). Non-canonical mTOR-Independent Role of DEPDC5 in Regulating GABAergic Network Development. *Current Biology*, *28*(12), 1924-1937.e5. https://doi.org/10.1016/j.cub.2018.04.061

Switon, K., Kotulska, K., Janusz-Kaminska, A., Zmorzynska, J., & Jaworski, J. (2017). Molecular neurobiology of mTOR. *Neuroscience*, *341*, 112–153. https://doi.org/10.1016/j.neuroscience.2016.11.017

Téllez-Zenteno, J. F., & Hernández-Ronquillo, L. (2012). A Review of the Epidemiology of Temporal Lobe Epilepsy. *Epilepsy Research and Treatment*, *2012*, 1–5. https://doi.org/10.1155/2012/630853

Tsokas, P., Ma, T., Iyengar, R., Landau, E. M., & Blitzer, R. D. (2007). Mitogen-activated protein kinase upregulates the dendritic translation machinery in long-term potentiation by controlling the mammalian target of rapamycin pathway. *Journal of Neuroscience*, *27*(22), 5885–5894. https://doi.org/10.1523/JNEUROSCI.4548-06.2007

Valente, P., Casagrande, S., Nieus, T., Verstegen, A. M. J., Valtorta, F., Benfenati, F., & Baldelli, P. (2012). Site-specific synapsin I phosphorylation participates in the expression of post-tetanic potentiation and its enhancement by BDNF. *Journal of Neuroscience*, *32*(17), 5868–5879. https://doi.org/10.1523/JNEUROSCI.5275-11.2012

Valente, P., Castroflorio, E., Rossi, P., Fadda, M., Sterlini, B., Cervigni, R. I., … Benfenati, F. (2016). PRRT2 Is a Key Component of the Ca2+-Dependent Neurotransmitter Release Machinery. *Cell Reports*, *15*(1), 117–131. https://doi.org/10.1016/j.celrep.2016.03.005

Valente, P., Orlando, M., Raimondi, A., Benfenati, F., & Baldelli, P. (2016). Fine Tuning of Synaptic Plasticity and Filtering by GABA Released from Hippocampal Autaptic Granule Cells. *Cerebral Cortex*, *26*(3), 1149–1167. https://doi.org/10.1093/cercor/bhu301

Wang, Y., Barbaro, M. F., & Baraban, S. C. (2006). A role for the mTOR pathway in surface expression of AMPA receptors. *Neuroscience Letters*, *401*(1–2), 35–39. https://doi.org/10.1016/j.neulet.2006.03.011

Way, S. W., Rozas, N. S., Wu, H. C., Mckenna Iii, J., Reith, R. M., Hashmi, S. S., … Gambello, M. J. (n.d.). The differential effects of prenatal and/or postnatal rapamycin on neurodevelopmental defects and cognition in a neuroglial mouse model of tuberous sclerosis complex. https://doi.org/10.1093/hmg/dds156

Yang, S. B., Tien, A. C., Boddupalli, G., Xu, A. W., Jan, Y. N., & Jan, L. Y. (2012). Rapamycin ameliorates age-dependent obesity associated with increased mTOR signaling in hypothalamic POMC neurons. *Neuron*, *75*(3), 425–436. https://doi.org/10.1016/j.neuron.2012.03.043

Yuskaitis, C. J., Jones, B. M., Wolfson, R. L., Super, C. E., Dhamne, S. C., Rotenberg, A., … Poduri, A. (2018). A mouse model of DEPDC5-related epilepsy: Neuronal loss of Depdc5 causes dysplastic and ectopic neurons, increased mTOR signaling, and seizure susceptibility. *Neurobiology of Disease*, *111*(December 2017), 91–101. https://doi.org/10.1016/j.nbd.2017.12.010

Yuskaitis, C. J., Rossitto, L. A., Gurnani, S., Bainbridge, E., Poduri, A., & Sahin, M. (2019). Chronic mTORC1 inhibition rescues behavioral and biochemical deficits resulting from neuronal Depdc5 loss in mice. *Human Molecular Genetics*, *28*(17), 2952–2964. https://doi.org/10.1093/hmg/ddz123

Zhang, J., Ji, F., Liu, Y., Lei, X., Li, H., Ji, G., … Jiao, J. (2014). Ezh2 regulates adult hippocampal neurogenesis and memory. *Journal of Neuroscience*, *34*(15), 5184–5199. https://doi.org/10.1523/JNEUROSCI.4129-13.2014

10. Appendix

Articles published by Maria Sabina Cerullo during the PhD course.

De Fusco A*, **Cerullo MS*,** Marte A, Michetti C, Romei A, Castroflorio E, Baulac S, Benfenati F. Acute knockdown of Depdc5 leads to synaptic defects in mTOR-related epileptogenesis. Neurobiol Dis. 2020 Jun;139:104822. doi: 10.1016/j.nbd.2020.104822. Epub 2020 Feb 27. PMID: 32113911.

Esposito A, Falace A, Wagner M, Gal M, Mei D, Conti V, Pisano T, Aprile D, **Cerullo MS**, De Fusco A, Giovedì S, Seibt A, Magen D, Polster T, Eran A, Stenton SL, Fiorillo C, Ravid S, Mayatepek E, Hafner H, Wortmann S, Levanon EY, Marini C, Mandel H, Benfenati F, Distelmaier F, Fassio A, Guerrini R. Biallelic DMXL2 mutations impair autophagy and cause Ohtahara syndrome with progressive course. Brain. 2019 Dec 1;142(12):3876-3891. doi: 10.1093/brain/awz326. Erratum in: Brain. 2020 Feb 1;143(2):e16. PMID: 31688942.

Articles published by Maria Sabina Cerullo during the PhD course due to previous work.

Marcantoni A, **Cerullo MS**, Buxeda P, Tomagra G, Giustetto M, Chiantia G, Carabelli V, Carbone E. Amyloid Beta42 oligomers up-regulate the excitatory synapses by potentiating presynaptic release while impairing postsynaptic NMDA receptors. J Physiol. 2020 Jun;598(11):2183-2197. doi: 10.1113/JP279345. Epub 2020 May 14. PMID: 32246769.